

ADA 086091

12
LEVEL III

AD-E 430 462

AD

MEMORANDUM REPORT ARBRL-MR-03022

AERODYNAMIC PERFORMANCE OF PROJECTILES
WITH AXISYMMETRIC AND
NON-AXISYMMETRIC BOATAILS

Lyle D. Kayser
Walter B. Sturek

May 1980

DTIC
ELECTE
S JUL 1 1980 D
B



US ARMY ARMAMENT RESEARCH AND DEVELOPMENT COMMAND
BALLISTIC RESEARCH LABORATORY
ABERDEEN PROVING GROUND, MARYLAND

DDC FILE COPY
800

Approved for public release; distribution unlimited.

80 6 18 0 12

Destroy this report when it is no longer needed.
Do not return it to the originator.

Secondary distribution of this report by originating
or sponsoring activity is prohibited.

Additional copies of this report may be obtained
from the National Technical Information Service,
U.S. Department of Commerce, Springfield, Virginia
22151.

The findings in this report are not to be construed as
an official Department of the Army position, unless
so designated by other authorized documents.

*The use of trade names or manufacturers' names in this report
does not constitute endorsement of any commercial product.*

UNCLASSIFIED

SECURITY CLASSIFICATION OF THIS PAGE (When Data Entered)

REPORT DOCUMENTATION PAGE		READ INSTRUCTIONS BEFORE COMPLETING FORM
1. REPORT NUMBER MEMORANDUM REPORT ARBRL-MR-03022	2. GOVT ACCESSION NO. <i>AD 4086 09</i>	3. RECIPIENT'S CATALOG NUMBER
4. TITLE (and Subtitle) AERODYNAMIC PERFORMANCE OF PROJECTILES WITH AXISYMMETRIC AND NON-AXISYMMETRIC BOATTAILS	5. TYPE OF REPORT & PERIOD COVERED Final	
7. AUTHOR(s) Lyle D. Kayser Walter B. Sturek	6. CONTRACT OR GRANT NUMBER(s)	
9. PERFORMING ORGANIZATION NAME AND ADDRESS U.S. Army Ballistic Research Laboratory (ATTN: DRDAR-BLL) Aberdeen Proving Ground, Maryland 21005	10. PROGRAM ELEMENT, PROJECT, TASK AREA & WORK UNIT NUMBERS RDT&E 1L162618AH80	
11. CONTROLLING OFFICE NAME AND ADDRESS U.S. Army Armament Research & Development Command U.S. Army Ballistic Research Laboratory (ATTN: DRDAR-BL) Aberdeen Proving Ground, MD 21005	12. REPORT DATE May 1980	
14. MONITORING AGENCY NAME & ADDRESS (if different from Controlling Office)	13. NUMBER OF PAGES 61	
16. DISTRIBUTION STATEMENT (of this Report)	15. SECURITY CLASS. (of this report) Unclassified	
17. DISTRIBUTION STATEMENT (of the abstract entered in Block 20, if different from Report)	15a. DECLASSIFICATION/DOWNGRADING SCHEDULE	
18. SUPPLEMENTARY NOTES		
19. KEY WORDS (Continue on reverse side if necessary and identify by block number) Projectile Aerodynamics Non-Axisymmetric Projectile Non-Conical Boattails		
20. ABSTRACT (Continue on reverse side if necessary and identify by block number) Aerodynamics properties of projectile shapes with axisymmetric and non-axisymmetric boattail shapes are presented. The nonaxisymmetric boattail is formed by a number of flat surfaces. Three flat surfaces equally spaced would develop into a triangle at the base; all non-conical data in this report are for the three-surface, or triangular, boattail. Surface pressure measurements were obtained on the non-conical boattail and a comparison of these measurements to three-dimensional flow field computations for the same shape are reported. Inviscid computations on several axisymmetric shapes are compared to experimental		

UNCLASSIFIED

SECURITY CLASSIFICATION OF THIS PAGE(When Data Entered)

20. ABSTRACT (Continued)

data obtained on non-axisymmetric boattail shapes so that an evaluation of the non-axisymmetric boattail performance could be made. The non-axisymmetric shapes can have significant stability advantages over axisymmetric shapes and still retain the advantage of drag reduction by boattailing.

UNCLASSIFIED

SECURITY CLASSIFICATION OF THIS PAGE(When Data Entered)

TABLE OF CONTENTS

	<u>Page</u>
LIST OF ILLUSTRATIONS	5
LIST OF TABLES	6
I. INTRODUCTION	7
II. PROJECTILE GEOMETRIES	8
III. EXPERIMENTS	9
IV. COMPUTATIONS	9
V. RESULTS	11
VI. CONCLUSIONS	13
REFERENCES	15
APPENDIX	41
LIST OF SYMBOLS	57
DISTRIBUTION LIST	59

ACCESSION for	
NTIS	White Section <input checked="" type="checkbox"/>
DDC	Buff Section <input type="checkbox"/>
UNANNOUNCED	<input type="checkbox"/>
JUSTIFICATION _____	
BY	
DISTRIBUTION/AVAILABILITY CODES	
Dist.	AVAIL and/or SPECIAL
A	

LIST OF ILLUSTRATIONS

<u>Figure</u>			<u>Page</u>
1	Non-Conical Boattail Geometry		17
2	Secant-Ogive, Cylinder, Boattail Geometry		18
3	Projectile A Geometry		19
4	Projectile B Geometry		20
5	M549 Geometry, c.g. = 3.5		21
6	Pressure Tap Locations		22
7	Circumferential Pressure Distribution, SOCBT-NC, Orientation A		23
a.	M = 2.0, Z/D = 5.25		23
b.	M = 2.0, Z/D = 5.50		24
c.	M = 2.0, Z/D = 5.75		25
d.	M = 3.0, Z/D = 5.50		26
e.	M = 2.0, Z/D = 5.50, Plotted Radially		27
f.	M = 3.0, Z/D = 5.50, Plotted Radially		28
8	Circumferential Pressure Distribution, SOCBT-NC, Orientations A and B		29
9	Longitudinal Pressure Distribution, SOCBT-NC, Orientation A		30
a.	M = 2.0, α = 2.5		30
b.	M = 3.0, α = 2.5		31
10	M549 Static Stability		32
a.	C_{N_a}		32
b.	C_{m_a}		33
11	SOCBT Static Stability		34
a.	C_{N_a}		34
b.	C_{m_a}		35

LIST OF ILLUSTRATIONS (Continued)

<u>Figure</u>		<u>Page</u>
12	Projectile A Static Stability	36
a.	C_{N_a}	36
b.	C_{m_a}	37
13	Projectile B Static Stability	38
a.	C_{N_a}	38
b.	C_{m_a}	39
14	Effect of Boattail Length on the Performance of Projectile A	40

LIST OF TABLES

<u>Table</u>		<u>Page</u>
1	Pressure Tap Location for the SOC and SOCBT-NC Models . .	16
2	Summary of Test Conditions for the NSWC Pressure Tests . .	16

I. INTRODUCTION

Recent studies have demonstrated that significant improvements in aerodynamic performance of projectiles can be achieved through the use of non-axisymmetric boattail shapes. The terms non-axisymmetric, non-conical, and unconventional are used interchangeably in this report. The non-axisymmetric boattail shape is simply a boattail formed by a number of flat surfaces as opposed to the conventional axisymmetric conical boattail. For example, three flat surfaces equally spaced would develop into a triangular base as shown in Figure 1. All non-axisymmetric boattail shapes considered in this report are for the three-surface triangular type boattail. Platou^{1,2,3,4} has considered non-axisymmetric boattail shapes and has demonstrated that projectile stability can be improved while still retaining the advantages of drag reduction through non-conical boattailing. For spinning projectiles, the boattail surfaces must be twisted at the same rate as the rifling twist. A resulting benefit of this twist is a reduction of the Magnus moment.

The objective of this study was to determine to what extent the existing computational capability can be used for determining the flow field over non-axisymmetric shapes. This study reports surface pressure measurements obtained on a non-spinning non-conical boattail and a comparison of these measurements to three-dimensional flow field computations of wall pressure for the same shape; since the pressure model was non-spinning, there was no twist in the boattail flats. Inviscid computations of static stability data on several axisymmetric shapes are compared to experimental free-flight data of spinning non-conical projectile shapes. One of these axisymmetric shapes has the same cross sectional area at each longitudinal station and is referred to as the equivalent-area shape. Model spin would have no effect, and need not be considered, in inviscid computations for axisymmetric shapes.

1. A. S. Platou, "An Improved Projectile Boattail," USA ARRADCOM Ballistic Research Laboratory Memorandum Report No. 2395, July 1974, AD 785520.
2. A. S. Platou, "An Improved Projectile Boattail. Part II," USA ARRADCOM Ballistic Research Laboratory Report No. 1866, March 1976, AD A024073.
3. A. S. Platou, "An Improved Projectile Boattail. Part III," USA ARRADCOM Ballistic Research Laboratory Memorandum Report No. 2644, July 1976, AD B012781L.
4. A. S. Platou, "An Improved Projectile Boattail. Part IV," USA ARRADCOM Ballistic Research Laboratory Memorandum Report No. ARBRL-MR-02825, April 1978, AD B027520L.

II. PROJECTILE GEOMETRIES

The basic projectile geometries for which experimental and theoretical (computational) data are presented are shown in Figures 1-5. There are variations to these geometries which are described below along with associated abbreviations:

- a. SOCBT
 - Secant-ogive-cylinder with a one caliber, 7° conical boattail, $l/d = 6.0$, Figure 2.
- SOC
 - Secant-ogive-cylinder, $l/d = 6.0$, as shown in Figure 2 but with 0° boattail.
- SOCBT-NC
 - Secant-ogive-cylinder, with a one caliber, 7° , 3-surface, non-conical boattail, $l/d = 6.0$. The boattail of Figure 1 on the forebody of Figure 2.
- b. Proj A
 - Projectile A with a 2.04 caliber, 7° non-conical boattail, $l/d = 6.47$, Figure 3.
 - Proj A-C
 - Figure 3 forebody with a 2.04 caliber, 7° conical boattail, $l/d = 6.47$.
 - Proj A-CYL - Projectile A forebody with 0° boattail, $l/d = 6.47$.
 - Proj A-Eq - Projectile A forebody with a 2.04 caliber axisymmetric boattail having the same cross sectional area at each longitudinal station as Proj A.
- c. Proj B
 - Projectile B with a 2.04 caliber, 7° non-conical boattail, $l/d = 6.71$, Figure 4.
 - Proj B-C
 - Projectile B with a 2.04 caliber, 7° conical boattail, $l/d = 6.71$.
 - Proj B-CYL - Projectile B with a 0° boattail, $l/d = 6.71$.
 - Proj B-Eq - Projectile B with a 2.09 caliber axisymmetric boattail having the same cross sectional area at each longitudinal station as Proj B, $l/d = 6.71$.
- d. M549
 - The 155mm M549 Artillery projectile, Figure 5.

Some minor modifications were made in the projectile shapes for computational purposes because the programs cannot currently handle fuze tip bluntness and rotating band discontinuities.

III. EXPERIMENTS

Surface pressure measurements were obtained on the secant-ogive-cylinder model with a 7° non-conical boattail (SOCBT-NC). Experimental results for other non-axisymmetric shapes were taken from References 1-4. The axial location of the pressure taps is given in Table 1 and the circumferential position of taps on the boattail is shown in Figure 6. Taps 1-7 on the ogive and cylinder were in line with taps 1-10 on the boattail. The pressure tests were conducted in the Supersonic Wind Tunnel No. 2 of the Naval Surface Weapons Center, White Oak Laboratory, Silver Spring, Maryland at Mach Numbers of 0.91, 1.75, 2.00, and 3.02. Data were recorded at 0, 1.0, 2.5, and 5.0 degrees angle of attack and at roll angles from 0 to 360 degrees in increments of five degrees. A summary of the test conditions is given in Table 2. Pressure tap No. 19 which is the most aft tap on the cylindrical portion of the boattail, Figure 6, would not leak check and did give incorrect results but data from all other taps appeared to be good. Experimental data for the M549 shape was taken from References 5 and 6 and the SOCBT data are taken from Reference 7.

IV. COMPUTATIONS

All computations in this study were obtained by the numerical technique developed by Sanders⁸ and is applicable to yawed, pointed bodies in supersonic flow. More specifically, the program was developed to treat the Magnus problem associated with spinning projectiles. The technique has been used successfully for many shapes at small angle of attack. The program uses MacCormack's⁹ shock capturing technique and is

5. R. Kline, W. R. Herrman, and V. Oskay, "A Determination of the Aerodynamic Coefficients of the 155mm, M549 Projectile," Picatinny Arsenal Technical Report No. 4764, November 1974, AD B002073L.
6. A. S. Platou, and G. I. T. Nielsen, "Some Aerodynamic Characteristics of the Artillery Projectile XM549," USA ARRADCOM Ballistic Research Laboratory Memorandum Report No. 2284, April 1973, AD 910093L.
7. C. J. Neitubica, and K. C. Opalka, "Supersonic Wind Tunnel Measurements of Static and Magnus Aerodynamic Coefficients for Projectile Shapes with Tangent and Secant Ogive Noses," USA ARRADCOM Ballistics Research Laboratory Memorandum Report No. 02991, February 1980, AD
8. B. R. Sanders, "Three-Dimensional, Steady, Inviscid Flow Field Calculations with Application to the Magnus Problem," PhD Dissertation, University of California, Davis, California, May 1974.
9. R. W. MacCormack, "The Effect of Viscosity in Hypervelocity Impact Cratering", AIAA Paper 69-364, 1969.

a second order scheme that uses a predictor-corrector method to solve the equations of motion. The computational procedure is as follows: (1) compute the inviscid flow over the body; (2) compute the boundary layer over the spinning body from the pressure distribution obtained by the inviscid computations; (3) modify the original body shape to account for boundary layer displacement thickness and recompute the inviscid flow over the new shape. Computations for this report used only the inviscid phase of the program and no boundary layer effects were computed.

A preliminary effort was made to compute the flow over the secant-cylinder model with the 3-surface non-conical boattail (SOCBT-NC). The same grid spacing that was used for the axisymmetric shapes was used for the non-conical shape. There were 36 grid points spaced circumferentially around the model in 10 degree increments. The grid was not forced to locate points at the corners formed by the intersection of the flat and cylindrical surfaces; to this extent, the non-conical boattail shape was approximated. The surface pressures were computed but were not integrated to obtain the aerodynamic coefficients since the objective was to compare computed pressures with pressure measurements obtained at the Naval Surface Weapons Center.

Inviscid computations were made on several axisymmetric shapes which are to be compared with experimental data from non-axisymmetric shapes. The intent of these comparisons is to give a measure of the effectiveness of the non-axisymmetric shapes. Comparisons are primarily of normal force and pitching moment data and past experience has shown that viscous effects on C_N , C_m are small for typical axisymmetric projectile shapes;

for this reason, the boundary layers were not computed. One of the axisymmetric shapes computed was the equivalent-area shape which has very nearly the same physical characteristics as the non-conical shapes. The geometry was chosen so that the equivalent-area shape would have the same cross sectional area at each longitudinal station. Equivalent-area boattail shapes were generated for Projectile A, Projectile B, and the SOTCBT-NC. Values of C_N , and C_m were obtained by

making computations at one degree angle of attack and assuming linearity in the range of zero to one degree.

For computational purpose, noses were extended to give a sharp tip and rotating bands were ignored.

V. RESULTS

Some of the tabulated pressure data obtained at the NSWC are presented in the Appendix. Data were acquired by rolling the model about the longitudinal axis. If we consider a model at angle of attack, a change in roll angle does not change the flow field of an axisymmetric shape, therefore the pressure distribution around the model is merely the pressure obtained from the different roll positions. For non-axisymmetric shapes the flow field does change with each roll position but is periodic every 120 degrees for a three surface non-conical boattail. The circumferential pressure distribution for a given orientation is obtained from data at three different roll angles at 120 degree intervals, e.g., $\phi = 0, 120, 240$; $\phi = 90, 210, 330$, etc. Tabulated data are presented for three model orientations: Orientation A, $\phi = 0$; orientation B, $\phi = 180^\circ$; orientation C, $\phi = 90^\circ$.

Figures 7a-f show the circumferential pressure distribution on the non-conical afterbody. There are not enough experimental points to define the pressure distribution completely; however, similarities between the experiment and the computation are readily apparent. Figures 7a, b, and c show the pressure distribution at three longitudinal stations on the boattail. The computational pressures are seen to show a sharp drop at the cylinder-flat intersection, and are most severe at the aft station. Such a sharp change was not found in the experimental values and this is interpreted as a boundary layer effect which tends to weaken the expansion over the surface discontinuity. Figure 7d is another circumferential pressure distribution at $M = 3.0$ and longitudinally midway on the boattail. Figures 7e and f are the same data as Figures 7b and d but plotted in polar coordinates; these figures help visualize the complex pressure distribution on the boattail. Figure 8 shows the pressure distribution for two different orientations of the non-conical boattail and Figures 9a and b show the longitudinal pressure distribution. The computation is seen to give excellent agreement over the nose and midsections which are axisymmetric segments of the model.

The three-step computational technique described in the previous section which takes into account the boundary layer displacement effect will probably not be useful for the non-axisymmetric shapes with sharp surface discontinuities. The reason for this is that errors in pressure distribution will not permit accurate computation of boundary layer development. The inviscid computations are, however, encouraging because the similarities between computation and experiment indicate the correct qualitative trends and provide encouragement that when viscous terms are added to the equations of fluid motion (Navier-Stokes Equations), flow over non-axisymmetric shapes will be computed more accurately.

Figure 10a and b compare inviscid computations with experimental data for the M549 shape. The agreement is good except that the trend of C_{N_a} from Reference 5 in the Mach number range of 2-3 is different.

Variations in Reynolds number are the reason for the range of data from Reference 6. Again, it should be pointed out that the experimental results are for a viscous flow over slightly blunted projectiles with rotating bands. Figures 11a and b compare the inviscid computations for the SOCBT model with wind tunnel data from Reference 7. The agreement is better than for the M549 and this is to be expected because the experimental and computational geometries are identical; however, the computations do not include viscous effects. These comparisons of theory and experiment provide confidence that the inviscid computations will give reasonably accurate static stability results for axisymmetric shapes. An "equivalent-area" shape was included in this comparison although no non-conical data were available. The stability of the equivalent-area shape falls between that of the conical and cylindrical shapes. The equivalent-area boattail is a curved convex shape similar to the ogive shapes considered by Karpov¹⁰. Karpov's data showed that the total drag for the ogive boattail shape is slightly greater than for a conical boattail at $M = 1.7$. The equivalent area shape, compared to the conventional conical shape, has improved stability but at the expense of slightly increased drag. These comparisons demonstrate that the equivalent-area shape is a realistic projectile shape but not necessarily an optimum shape.

Figure 12a and b compare aerodynamic static stability data on Projectile A with four variations in the boattail shape. Figure 12a shows the variations in normal force for the different shapes. The differences or increments in normal force are due to variations in boattail geometry and are therefore acting near the base; hence, an increased normal force provides a restoring moment and means an improved or greater static stability. Figure 12b compares values of C_{m_a} which

is a measure of the static stability - a smaller pitching moment (C_{m_a}) means increased static stability. The non-conical triangular boattail shape is seen to have the best stability characteristics while the pure conical boattail shape has the poorest stability. Comparison of the non-conical and conical boattail shapes may not be the most rational comparison because of different physical properties, never the less

10. B. C. Karpov, "The Effect of Various Boattail Shapes on Base Pressure and Other Aerodynamic Characteristics of a 7-caliber Long Body of Revolution at $M = 1.70$ ", USA ARRAUDCOM Ballistic Research Laboratory Report No. 1295, August 1965, AD 474352.

the conical boattail is widely used and the comparison shows that a substantial increase in stability can be achieved by the use of non-axisymmetric shapes. A more logical comparison for the non-conical shape is to compare it with the axisymmetric equivalent-area shape since both have the same volume, longitudinal weight distribution and very nearly the same moments of inertia. The non-conical shape is substantially more stable than the equivalent-area shape even though the equivalent-area shape is an improvement over the conical shape. The rather substantial discrepancy between the non-conical and the equivalent-area data illustrate that the equivalent area shape should not be used as an approximation to the non-conical shape. Perhaps the most important comparison in assessing the performance of the non-conical shape is to compare it with the straight cylindrical boattail afterbody shape. The cylindrical afterbody could be expected to provide an upper limit for the stability characteristics for a conventional axisymmetric projectile shape although the drag is expected to be higher than for boattail shapes. The non-conical boattail is seen to give better stability characteristics than the projectile with a straight cylindrical afterbody which implies that the non-conical effect is equivalent to providing some fin area or to flaring of the afterbody. Platou has shown that the non-conical shape has the usual benefit of drag reduction through boattailing and that by twisting of the flats to provide a slight corkscrew effect, the Magnus moment can be significantly reduced.

Figures 13a and 13b compare static stability data on Projectile B with three variations in boattail shape. The results are similar to those for Projectile A with the non-conical boattail shape showing a significant increase in stability.

Figure 14 shows the variation in normal force for various boattail lengths. The boattail effect is seen to be amplified with increasing length; it would appear that a non-conical boattail would have to be greater than one caliber in length to have significant aerodynamic advantages.

VI. CONCLUSIONS

1. For stability computations, the equivalent-area axisymmetric shape is not a good approximation to the non-conical boattail shape.
2. Three-dimensional inviscid computations over the non-conical boattail shape provide qualitative agreement with experimental measurements of wall pressure. However, it is felt that viscous effects must be included in order to yield results of acceptable accuracy.
3. The inviscid computations provide good longitudinal stability predictions for axisymmetric shapes.

4. These computations support the findings of Platou concerning the advantages of the non-conical boattail shapes and help quantify the effect of non-conical boattail.

5. The non-conical boattail shape provides significant stability advantages over axisymmetric shapes while still retaining drag reduction advantages of boattailing.

REFERENCES

1. A. S. Platou, "An Improved Projectile Boattail," USA ARRADCOM Ballistic Research Laboratory Memorandum Report No. 2395, July 1974, AD 785520.
2. A. S. Platou, "An Improved Projectile Boattail Part II," USA ARRADCOM Ballistic Research Laboratory Report No. 1866, March 1976, AD A024073.
3. A. S. Platou, "An Improved Projectile Boattail. Part III," USA ARRADCOM Ballistic Research Laboratory Memorandum Report No. 2644, July 1976, AD B012781L.
4. A. S. Platou, "An Improved Projectile Boattail. Part IV," USA ARRADCOM Ballistic Research Laboratory Memorandum Report No. ARBRL-MR-02826, April 1978, AD B027520L.
5. R. Kline, W. R. Herrmann, and V. Oskay, "A Determination of the Aerodynamic Coefficients of the 155mm, M549 Projectile," Picatinny Arsenal Technical Report No. 4764, November 1974, AD B002073L.
6. A. S. Platou, and G. I. T. Nielsen, "Some Aerodynamic Characteristics of the Artillery Projectile XMS49," USA ARRADCOM Ballistic Research Laboratory Memorandum Report No. 2284, April 1973, AD 910093L.
7. C. J. Nietubicz, and K. C. Opalka, "Supersonic Wind Tunnel Measurements of Static and Magnus Aerodynamic Coefficients for Projectile Shapes with Tangent and Secant Ogive Noses," USA ARRADCOM Ballistics Research Laboratory Memorandum Report No. 02991, February 1980.
8. B. R. Sanders, "Three-Dimensional, Steady, Inviscid Flow Field Calculations with Application to the Magnus Problem," PhD Dissertation, University of California, Davis, California, May 1974.
9. R. W. MacCormack, "The Effect of Viscosity in Hypervelocity Impact Cratering", AIAA Paper 69-364, 1969.
10. B. G. Karpov, "The Effect of Various Boattail Shapes on Base Pressure and Other Aerodynamic Characteristics of a 7-caliber Long Body of Revolution at $M = 1.70$," USA ARRADCOM Ballistic Research Laboratory Report No. 1295, August 1965, AD 474352.

Table 1. Pressure Tap Location for SOCBT-NC

<u>Taps</u>	<u>Distance From Nose</u> (Z/D)
1	0.89
2	1.56
3	2.22
4	2.79
5	3.13
6	3.56
7	4.22
8, 11, 14, 17	5.25
9, 12, 15, 18	5.50
10, 13, 16, 19	5.75

Table 2. Summary of Test Conditions for the NSWC Pressure Tests

<u>M</u>	<u>P_o - atm</u>	<u>T_o °K</u>	<u>Re_λ</u>
0.91	1.0	330	4.5×10^6
1.75	1.0	330	4.4×10^6
2.02	1.0	330	3.8×10^6
3.02	1.0	330	2.5×10^6

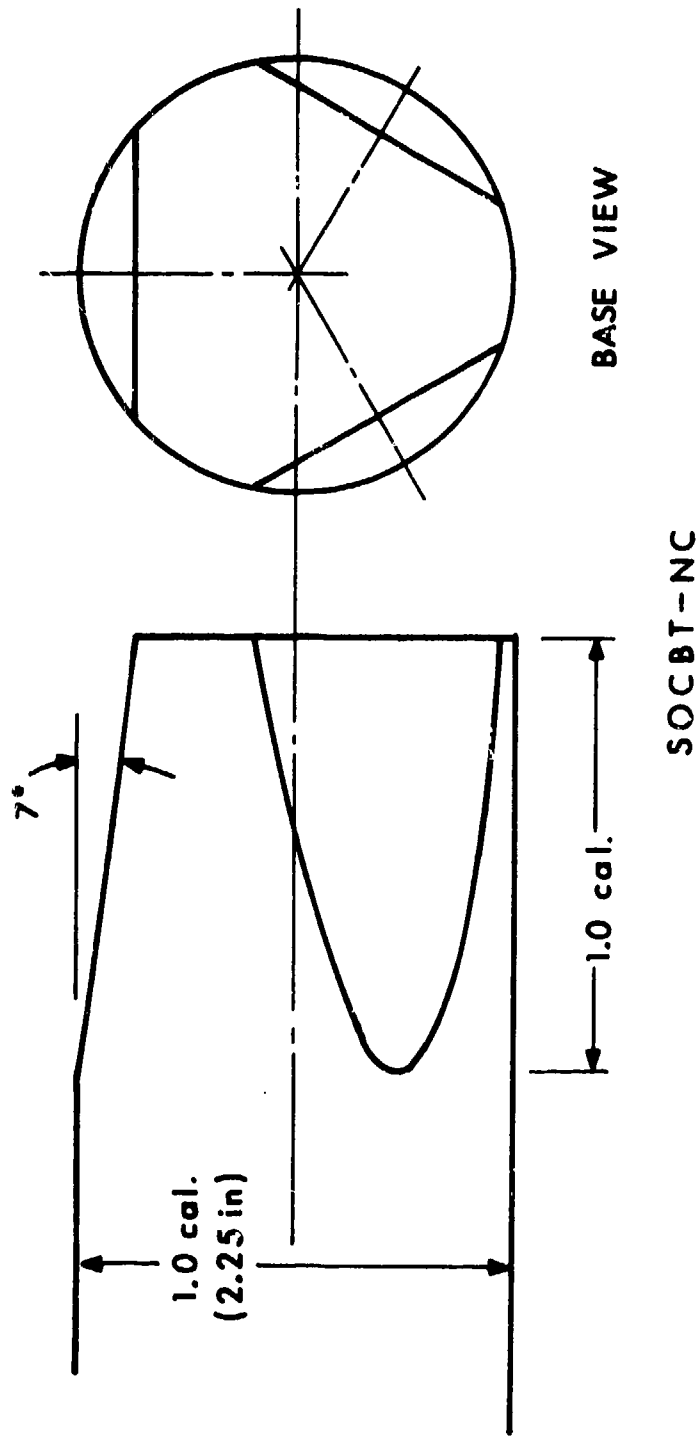


Figure 1. Non-Conical Boattail Geometry

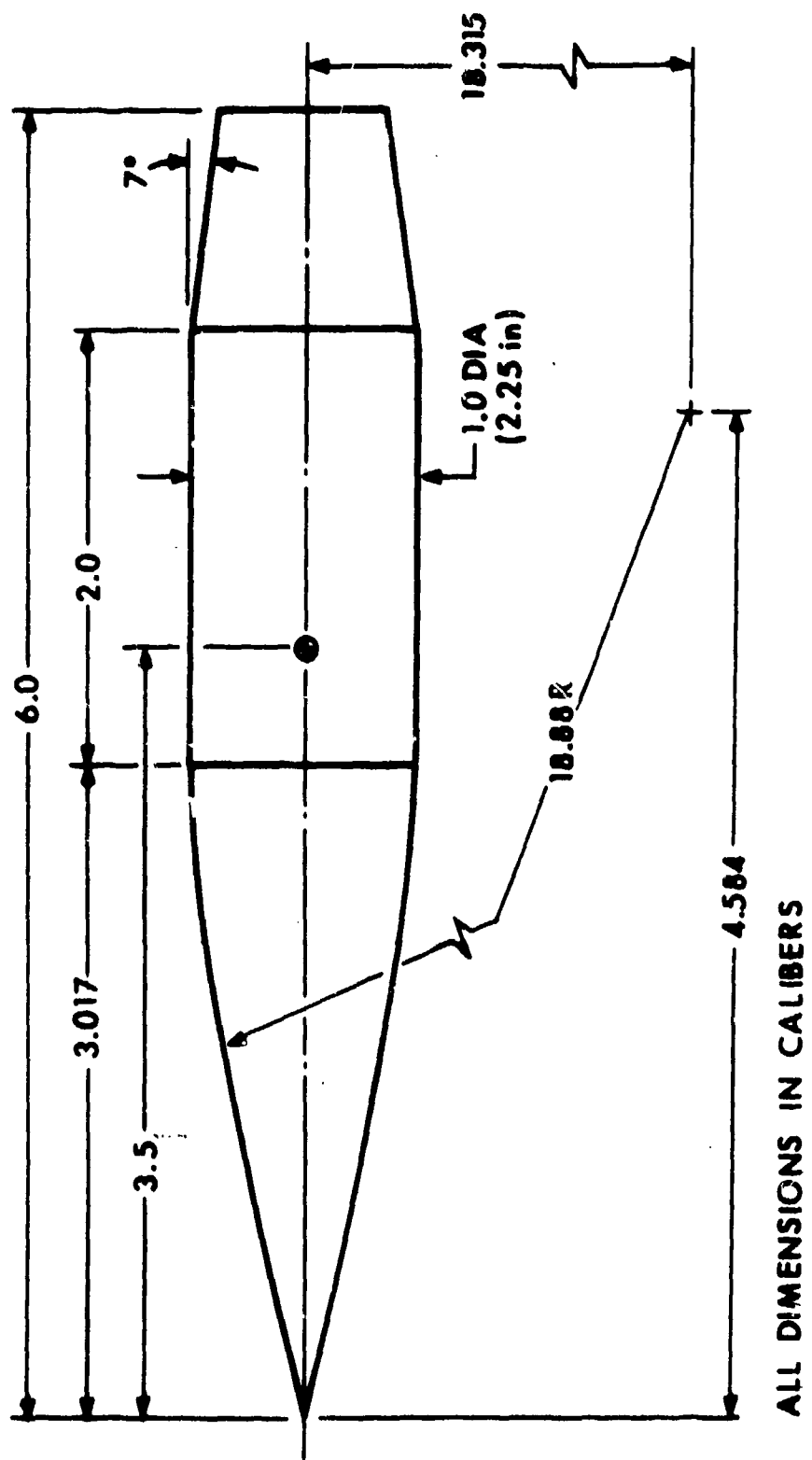


Figure 2. Secant-0give, Cylinder, Boattail Geometry

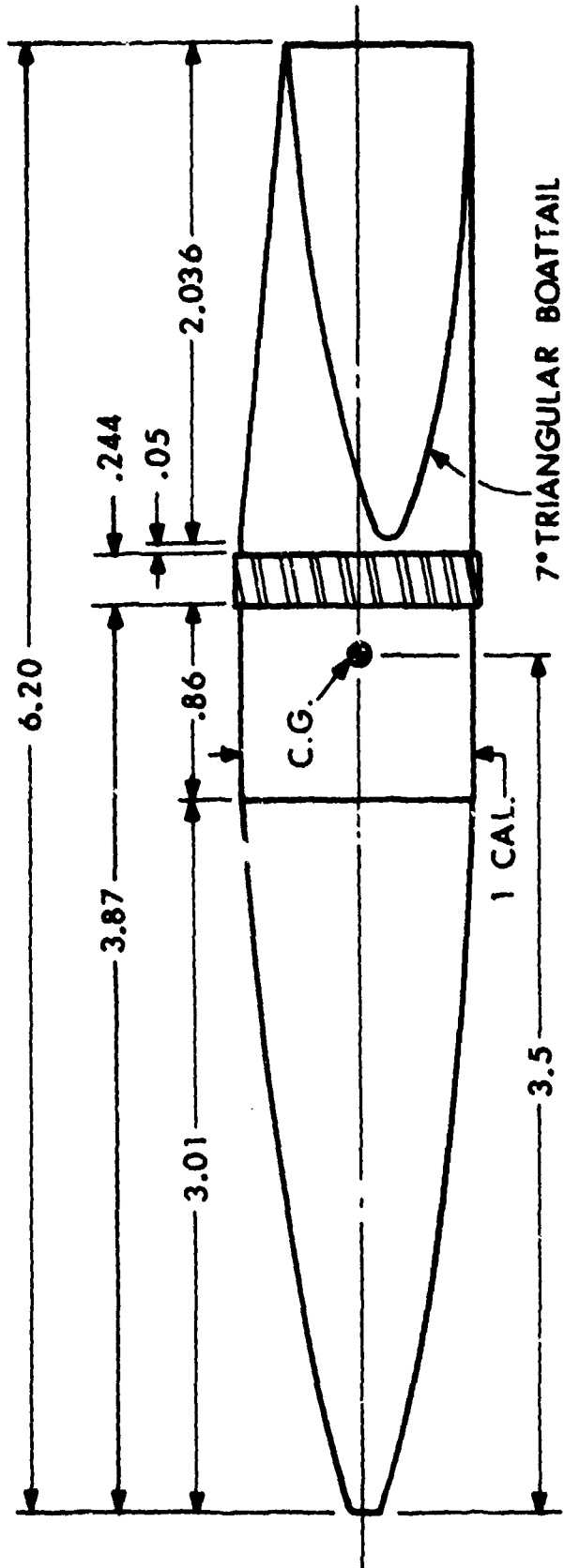


Figure 3. Projectile A Geometry

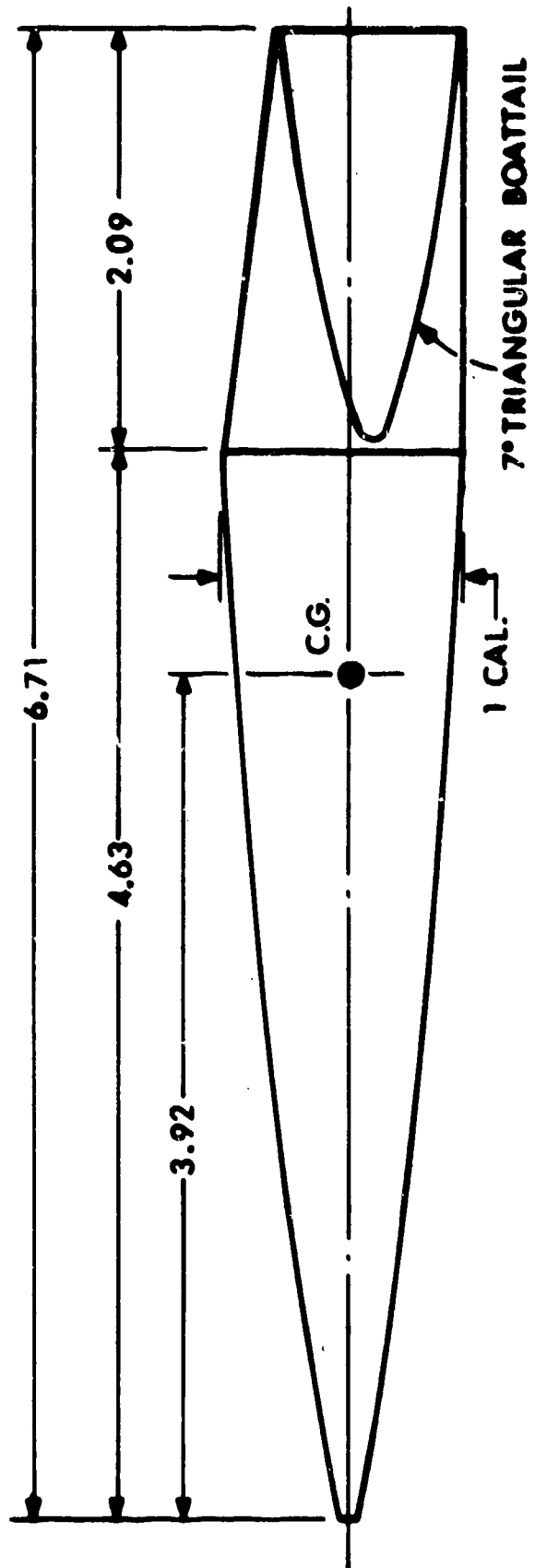


Figure 4. Projectile B Geometry

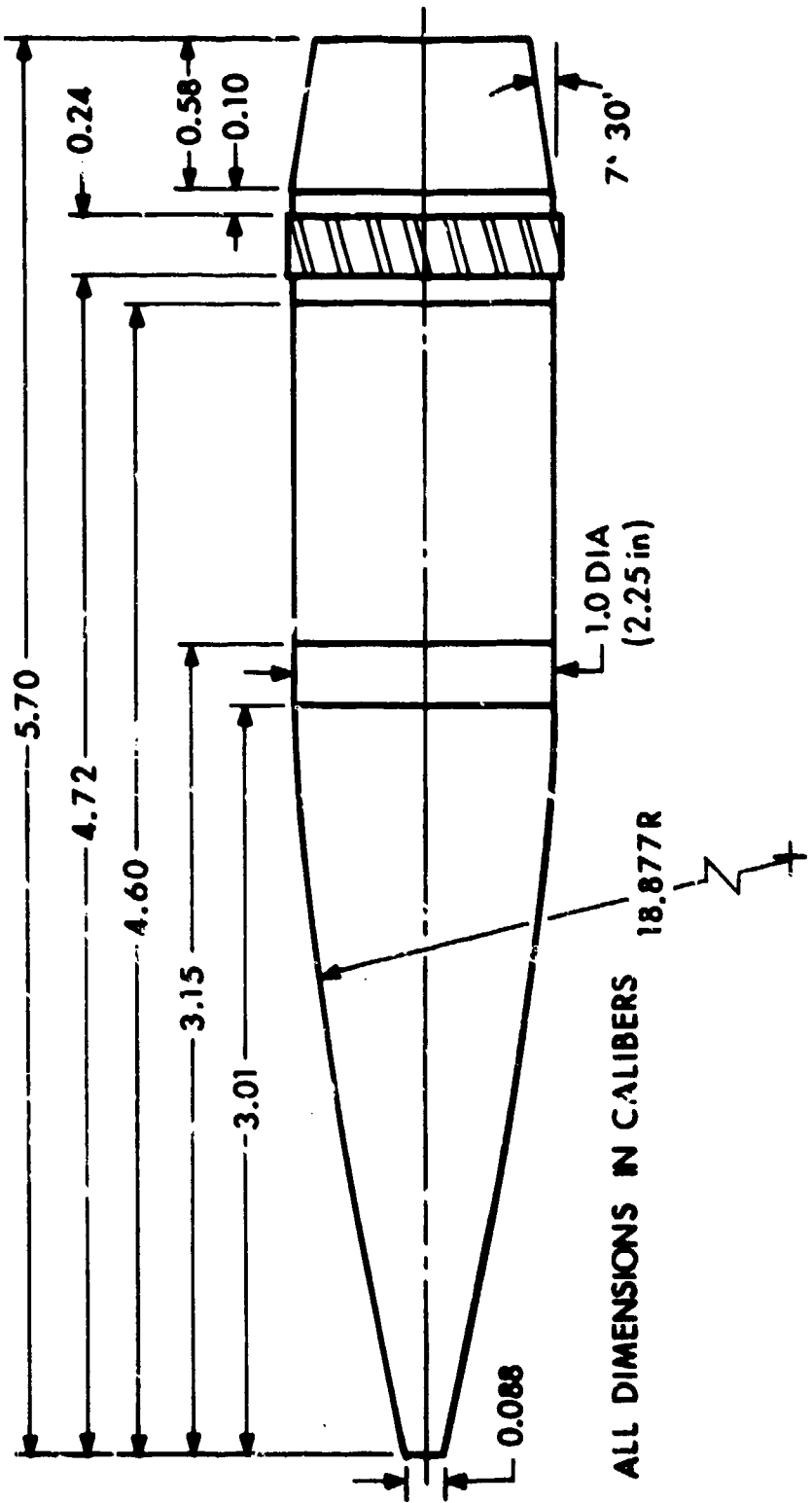


Figure 5. M549 Geometry, c.g. = 3.5

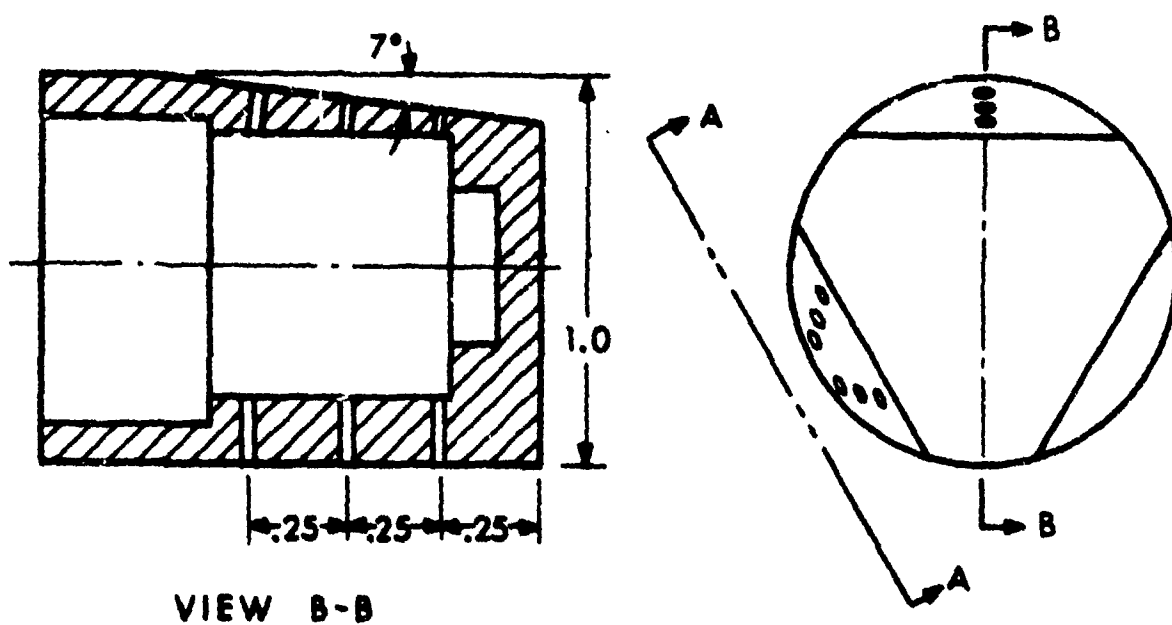
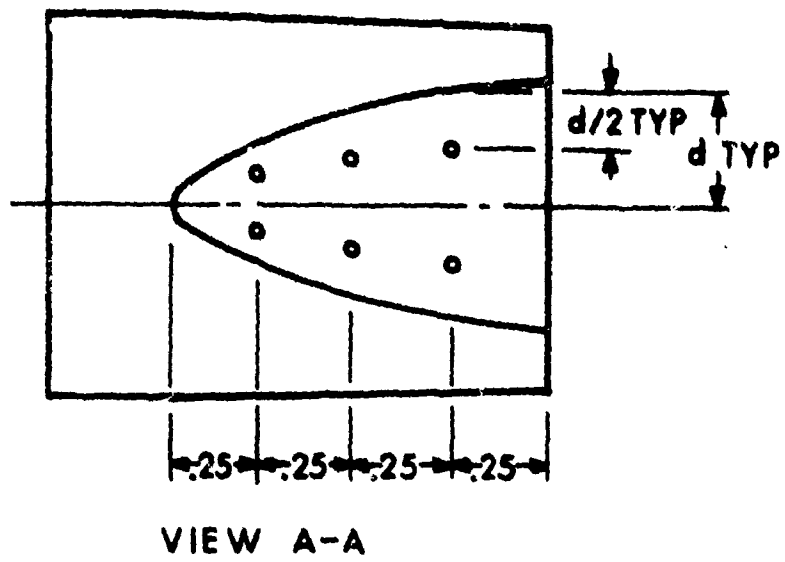


Figure 6. Pressure Tap Locations

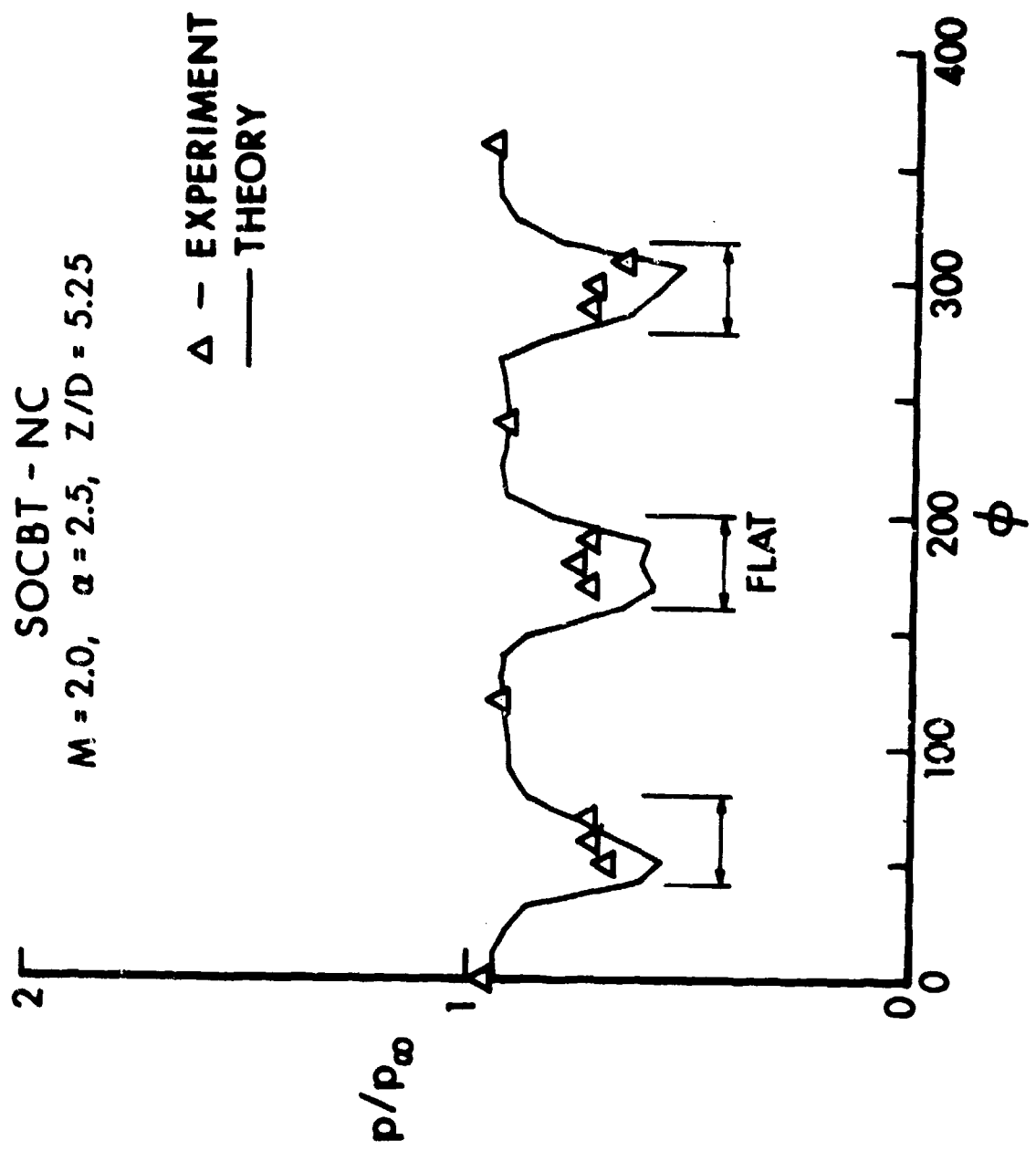


Figure 7. Circumferential Pressure Distribution, SOCBT-NC, Orientation A

a. $M = 2.0, Z/D = 5.25$

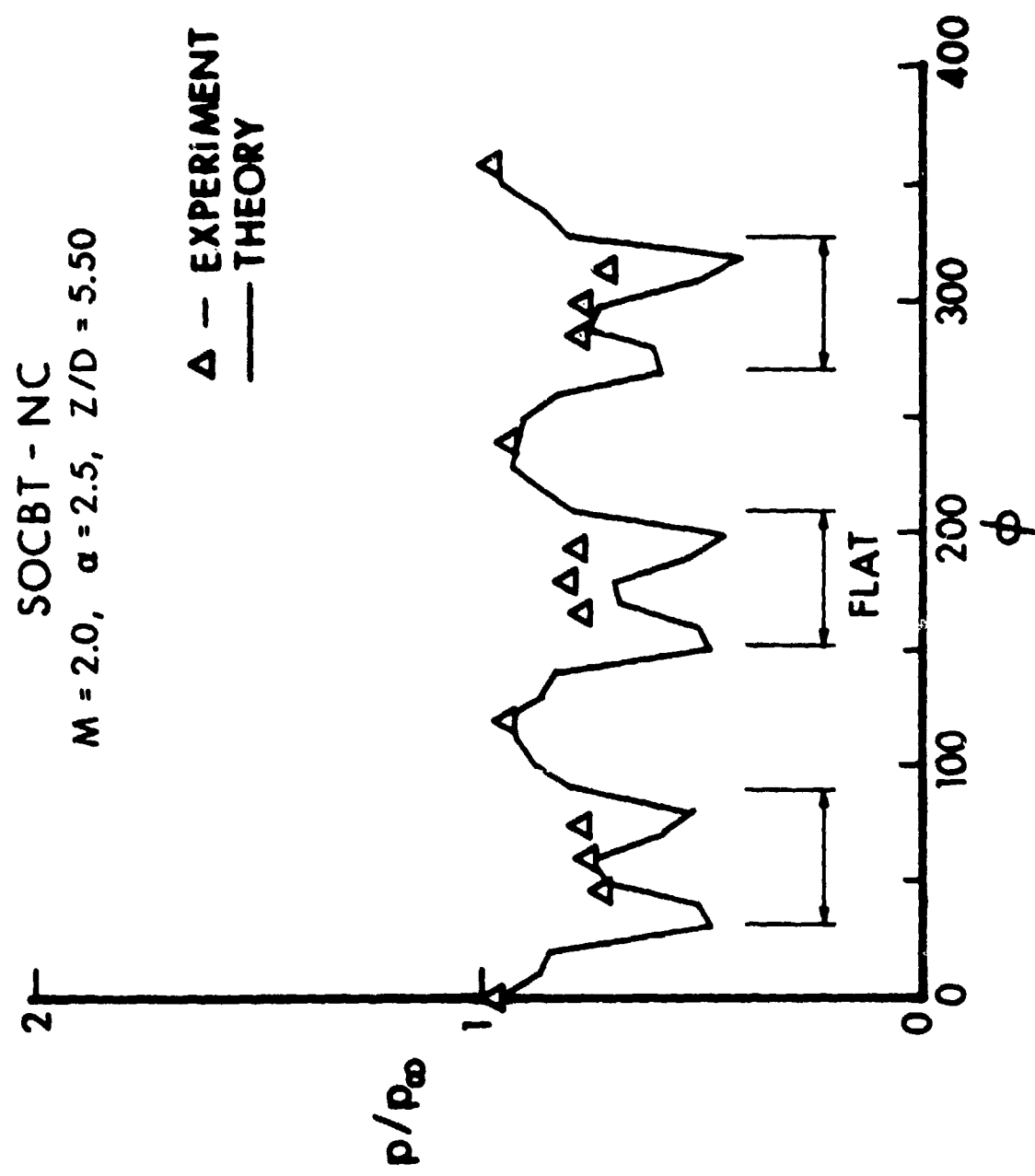


Figure 7. Continued
 b. $M = 2.0, Z/D = 5.50$

SOCBT - NC
 $M = 2.0, \alpha = 2.5, Z/D = 5.75$

Δ - EXPERIMENT
— THEORY

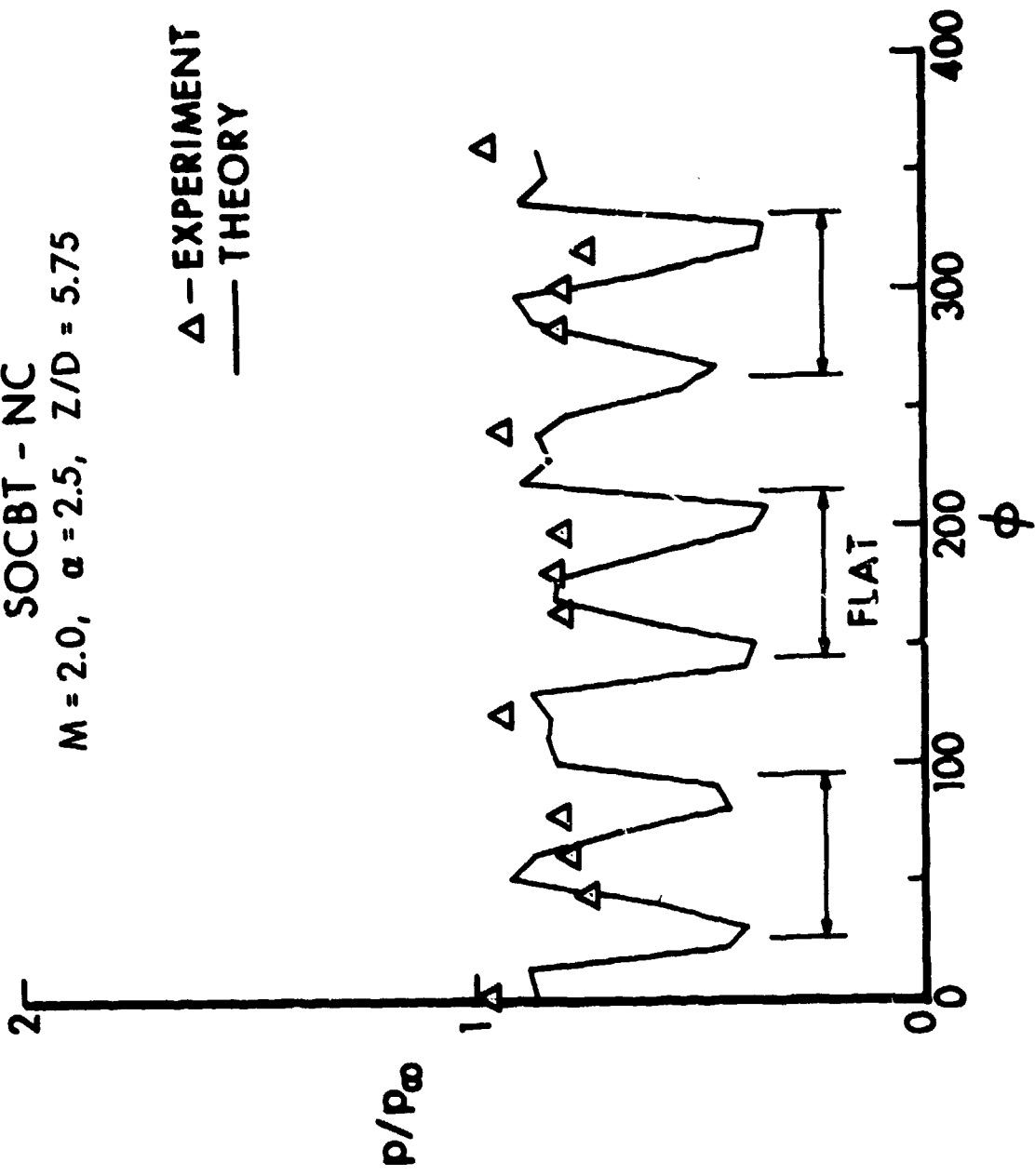


Figure 7. Continued
 $M = 2.0, Z/D = 5.75$

SOCBT - NC
 $M = 3.0, \alpha = 2.5, Z/D = 5.50$

Δ - EXPERIMENT
— THEORY

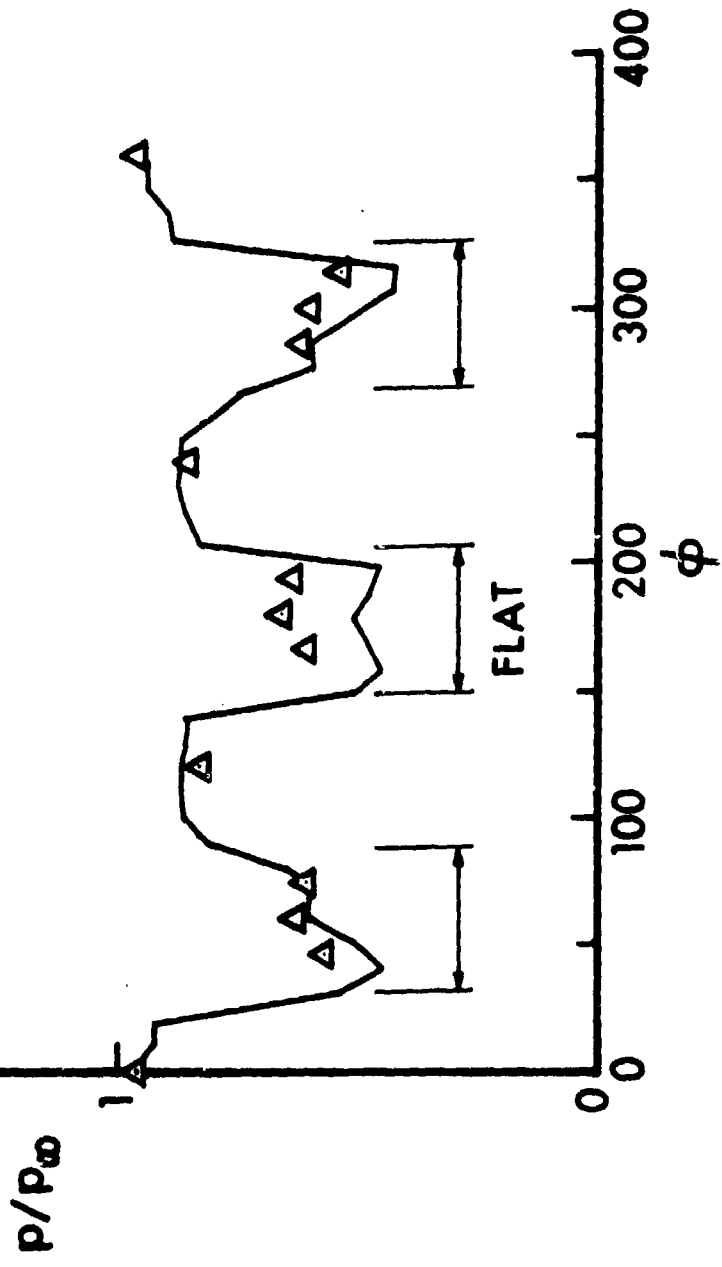


Figure 7. Continued
d. $M = 3.0, Z/D = 5.50$

SOCBT - NC
 $M = 2.0, \alpha = 2.5, Z/D = 5.50$

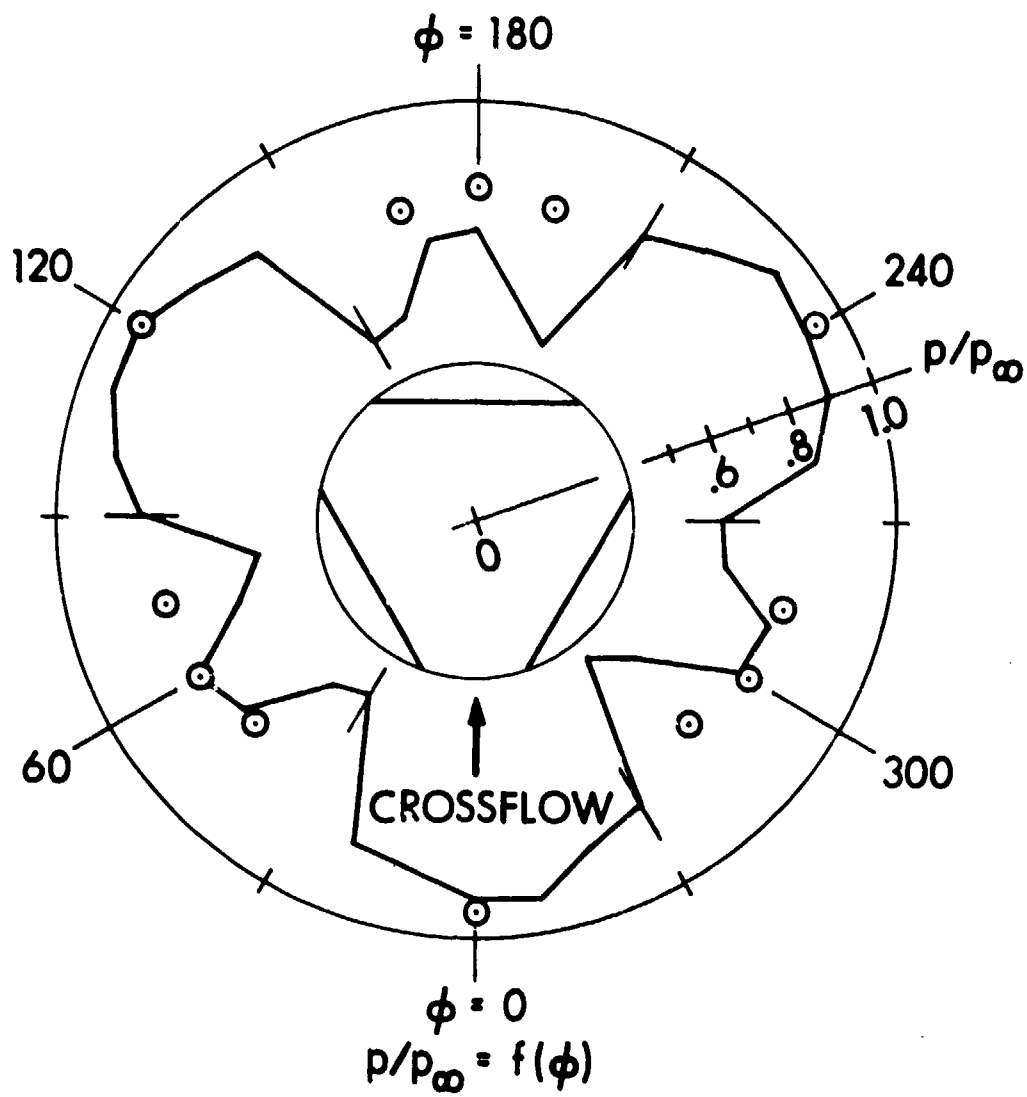


Figure 7. Continued

e. $M = 2.0, Z/D = 5.50$, Plotted Radially

SOCBT - NC
 $M = 3.0, \alpha = 2.5, Z/D = 5.50$

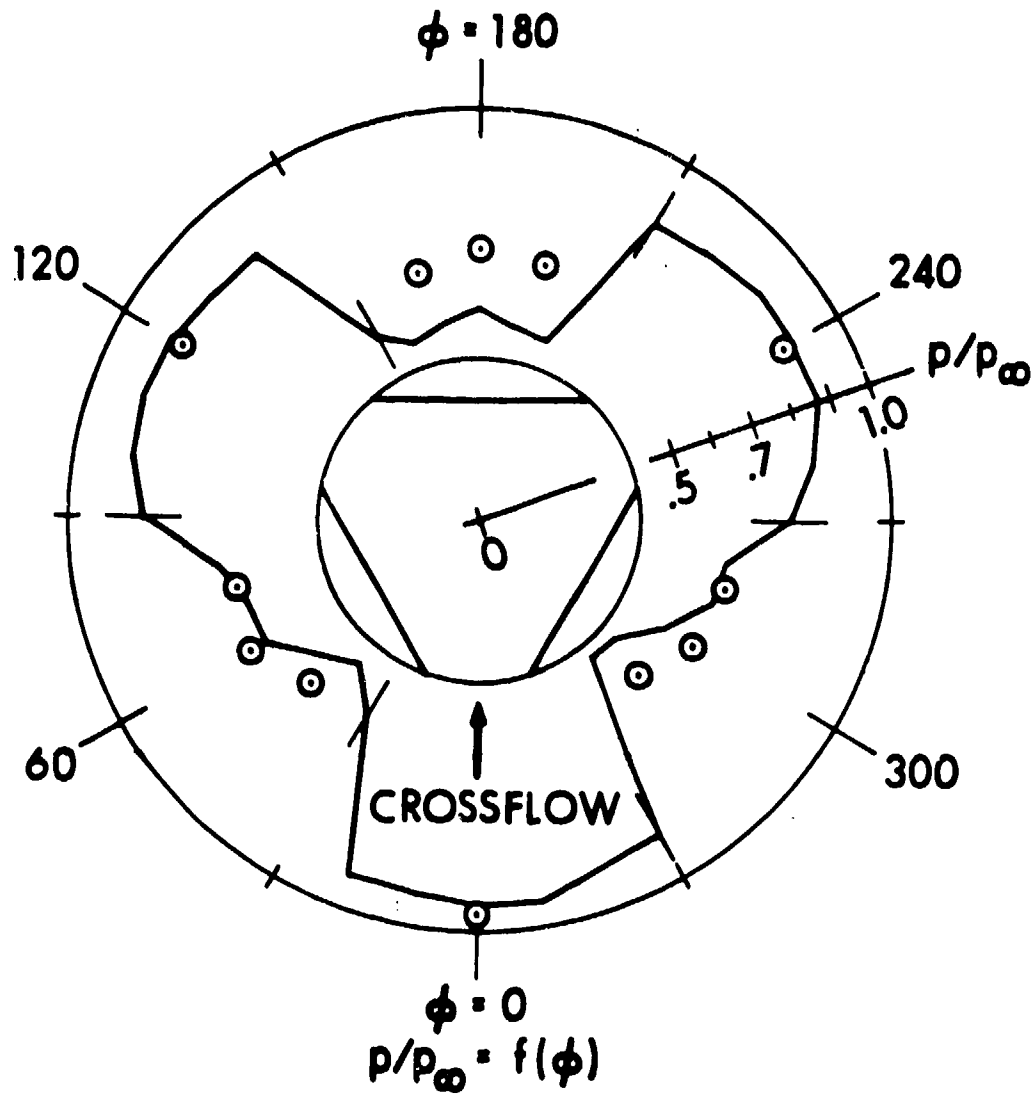


Figure 7. Continued

f. $M = 3.0, Z/D = 5.50$, Plotted Radially

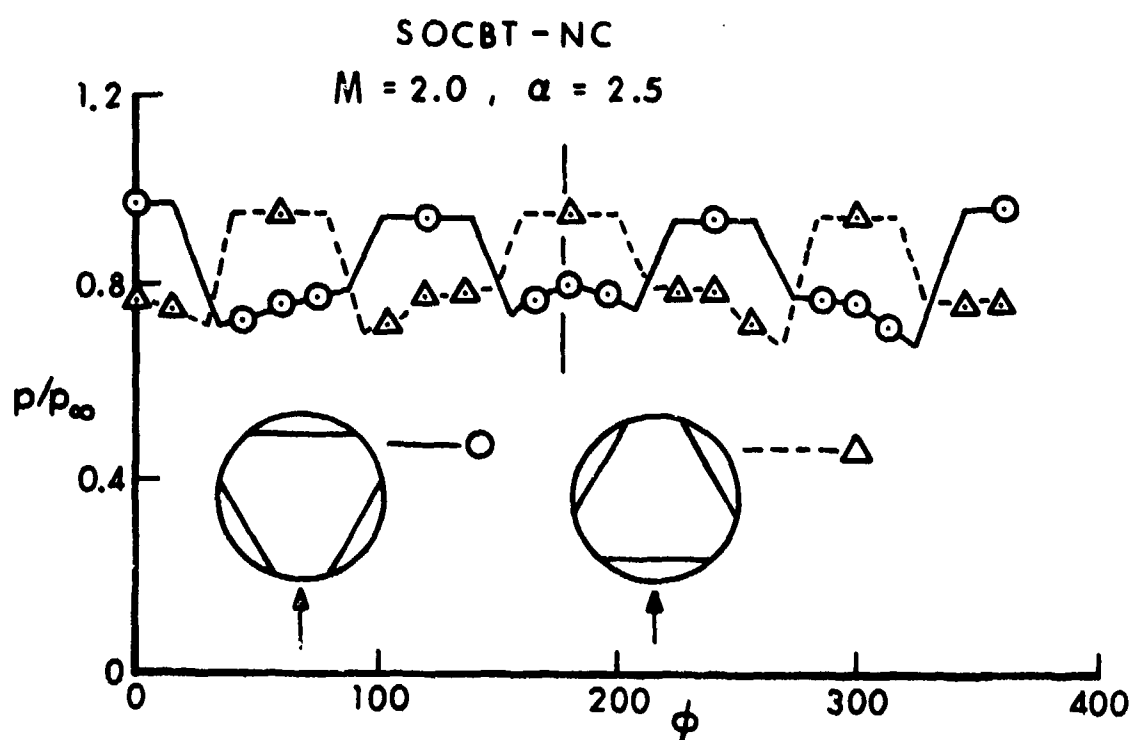


Figure 8. Circumferential Pressure Distribution, SOCBT-NC,
Orientations A and B

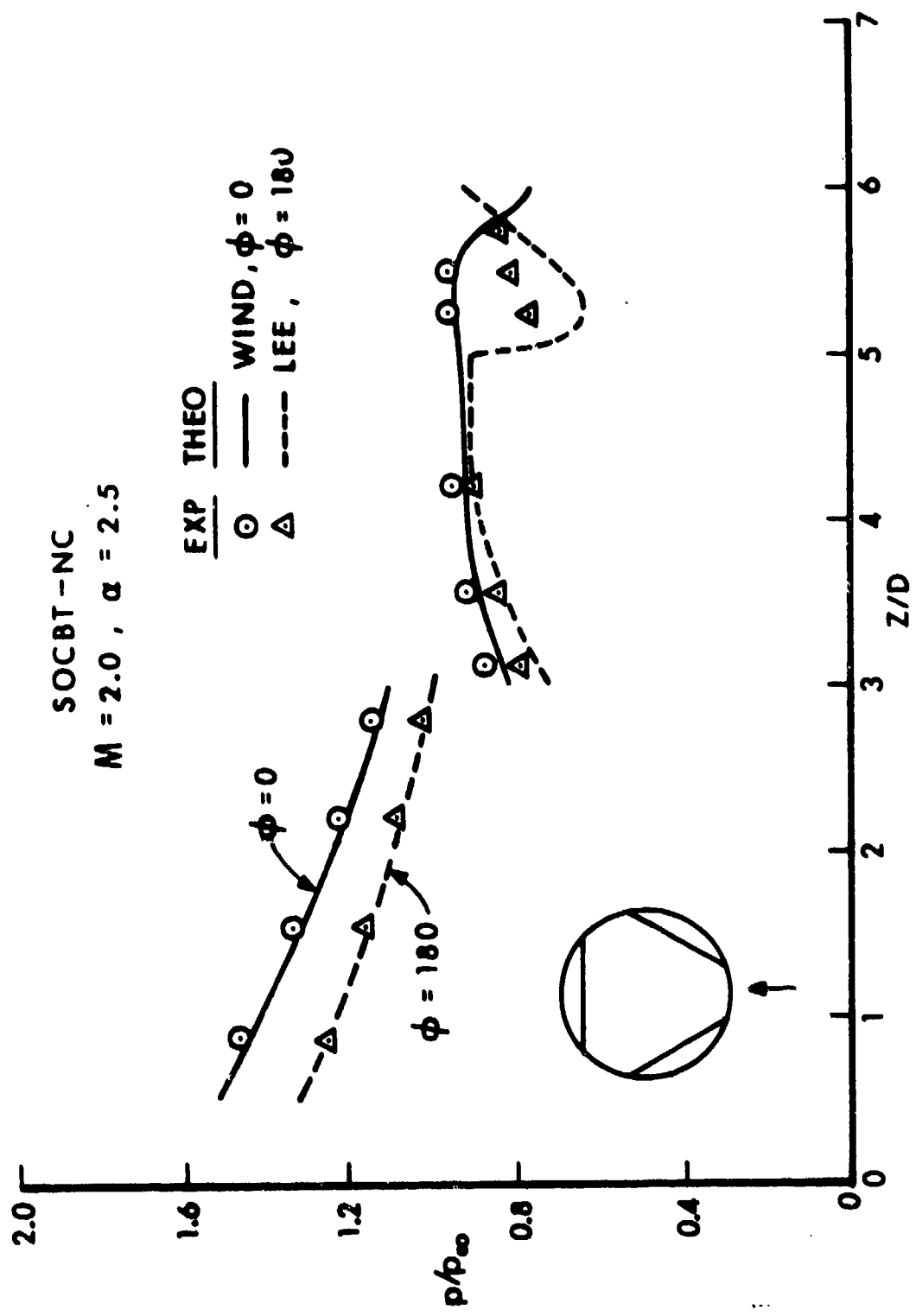


Figure 9. Longitudinal Pressure Distribution, SOCBT-NC, Orientation A

a. $M = 2.0, \alpha = 2.5$

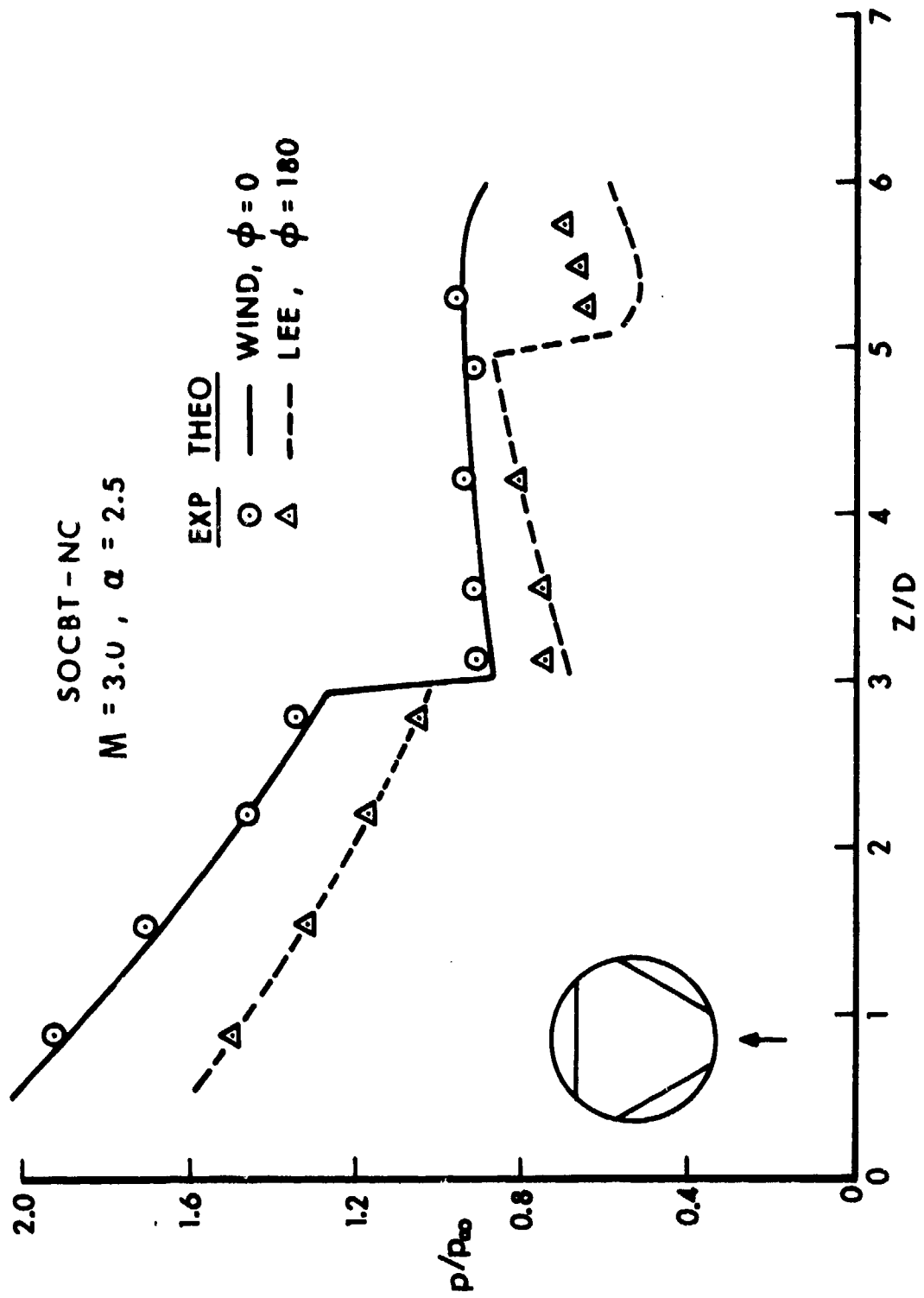


Figure 9. Continued
 b. $M = 3.0, \alpha = 2.5$

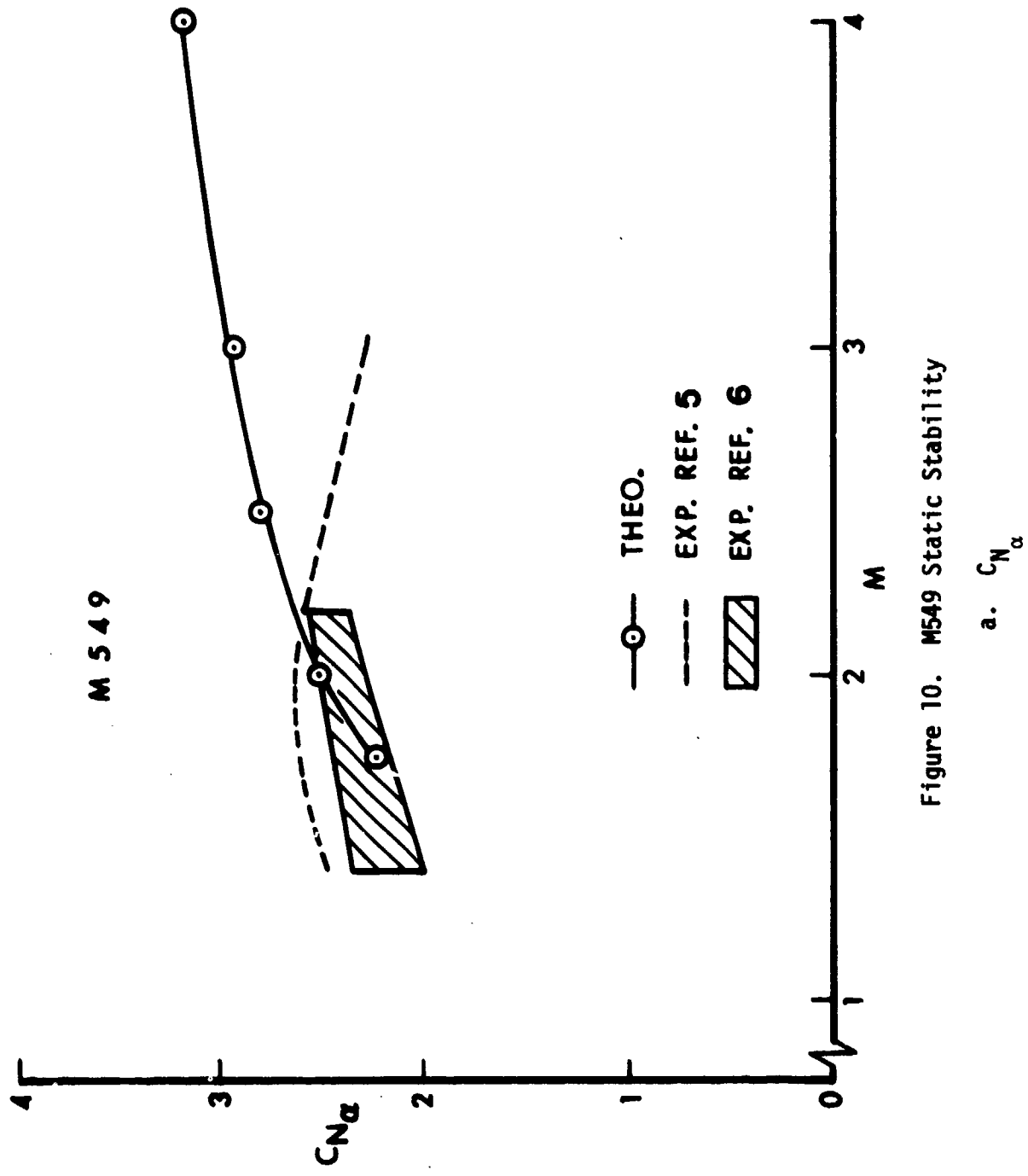


Figure 10. M549 Static Stability

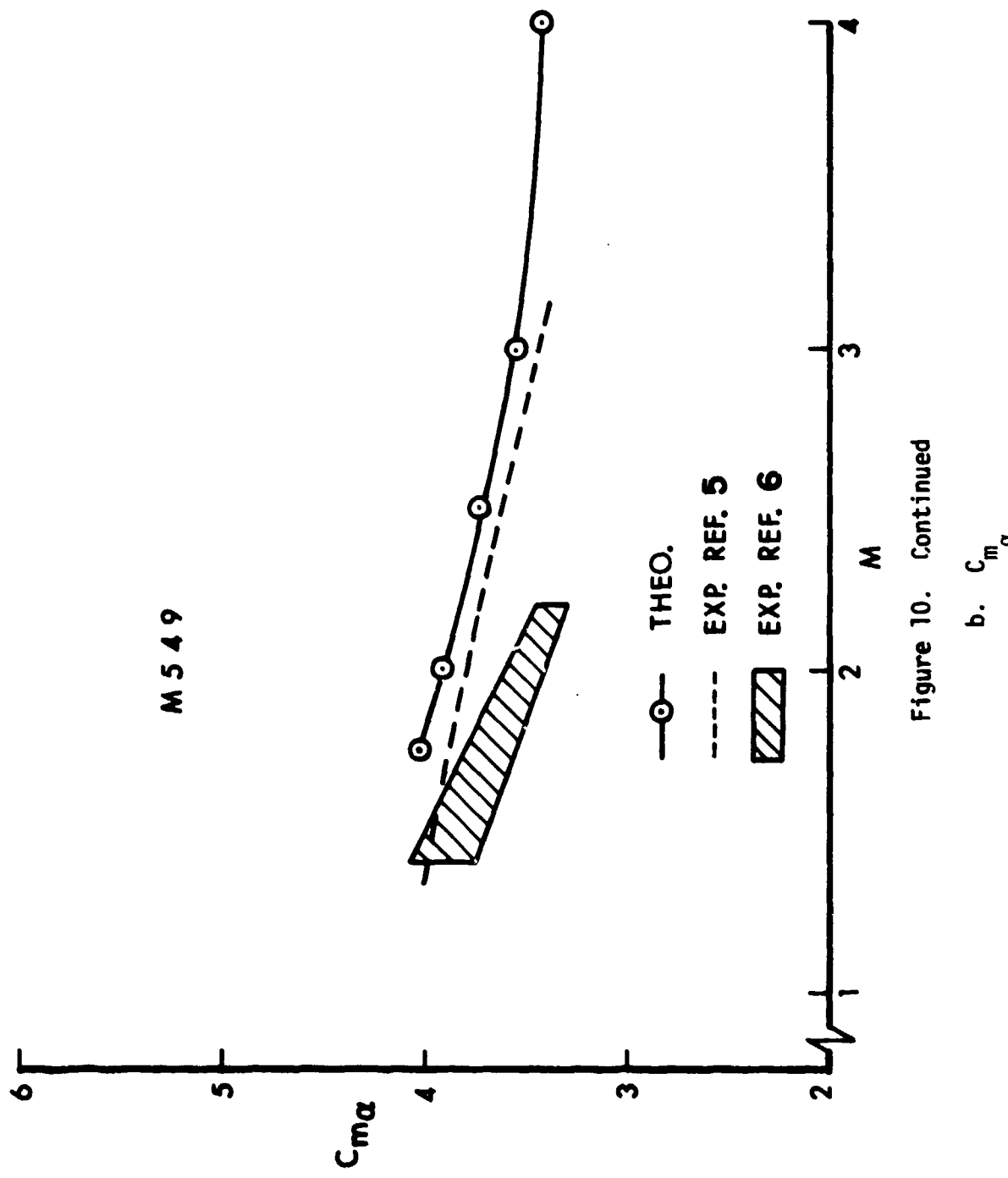
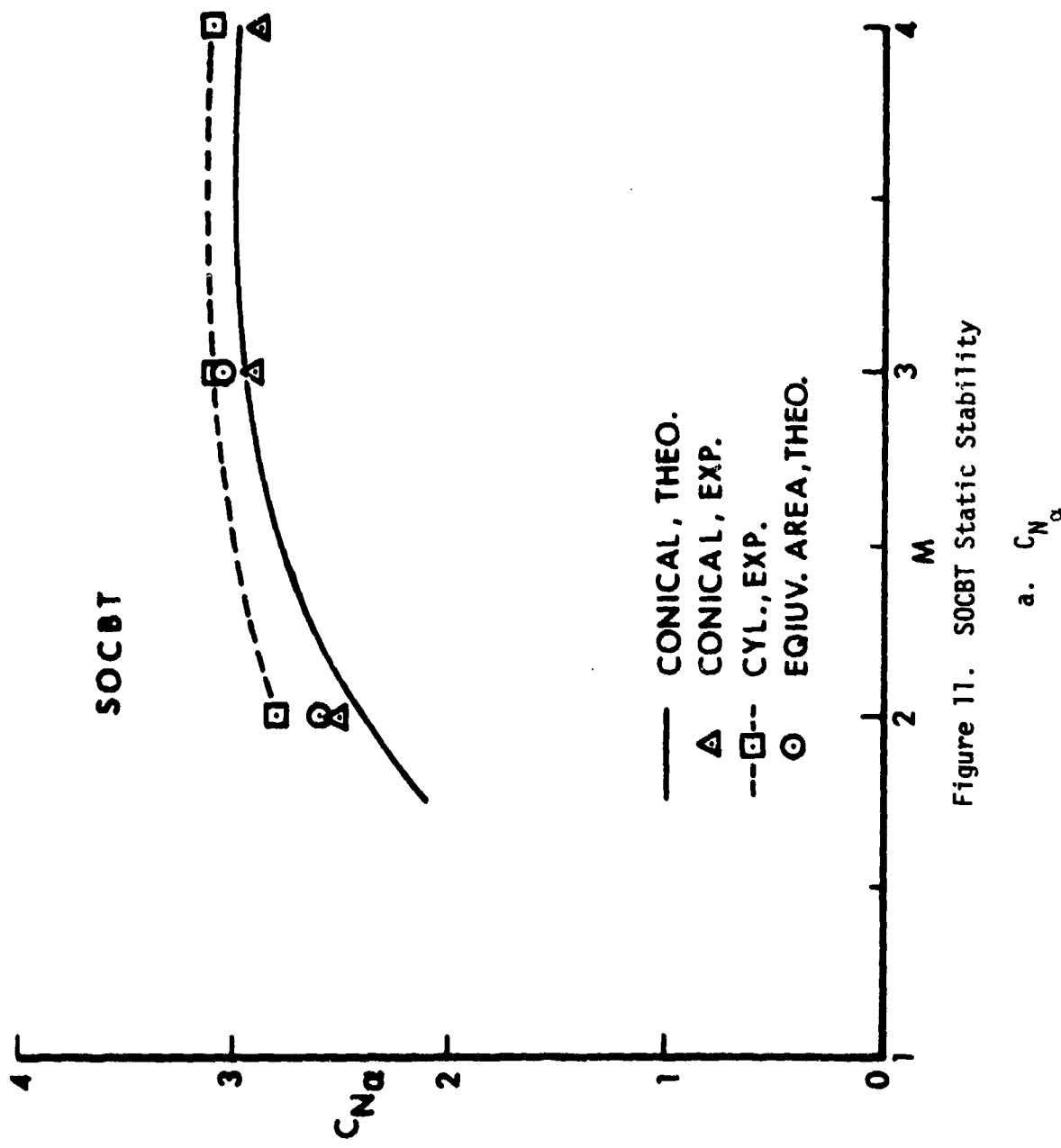


Figure 10. Continued
b. $C_{m\alpha}$



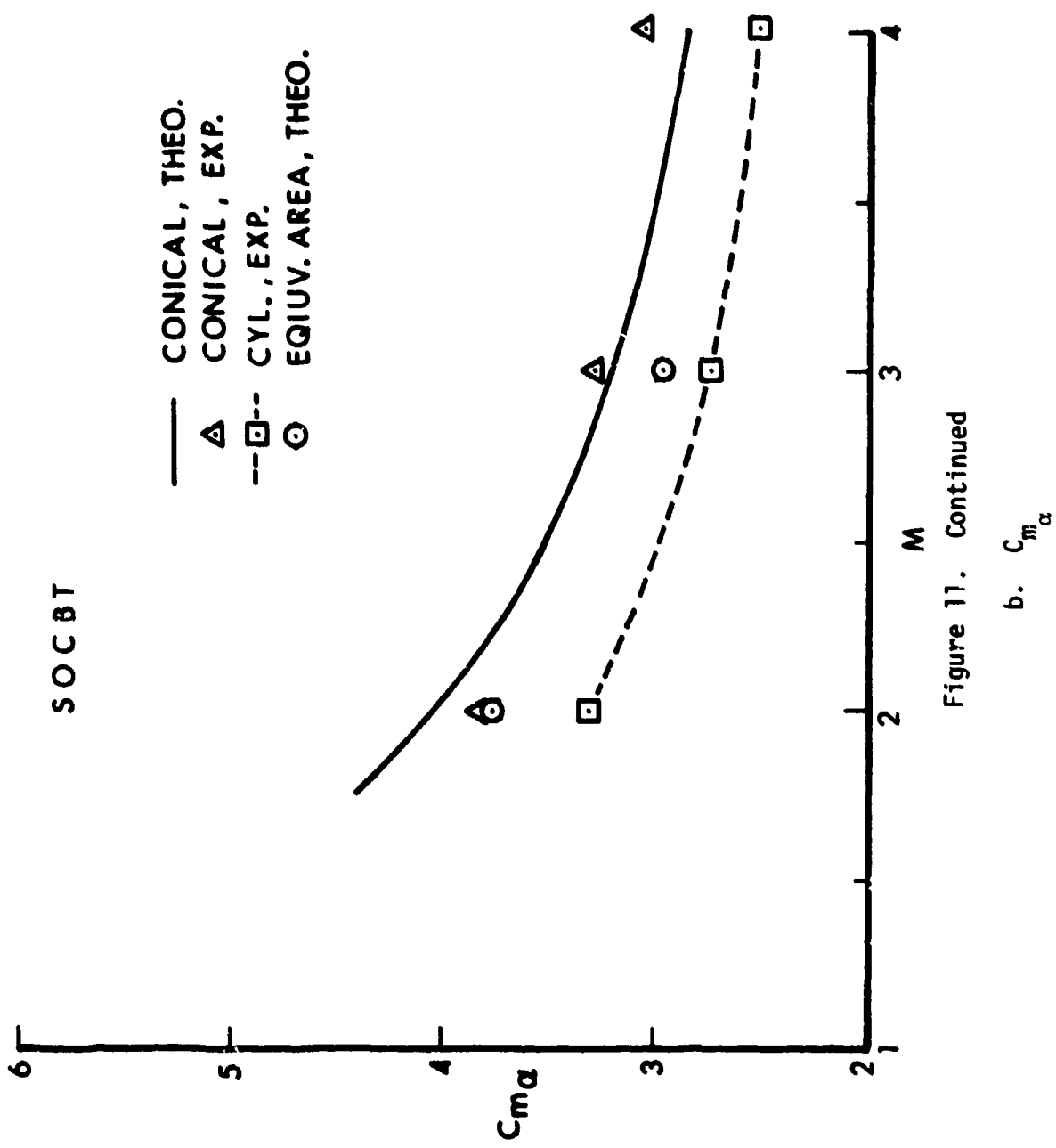


Figure 11. Continued

b. $C_{m\alpha}$

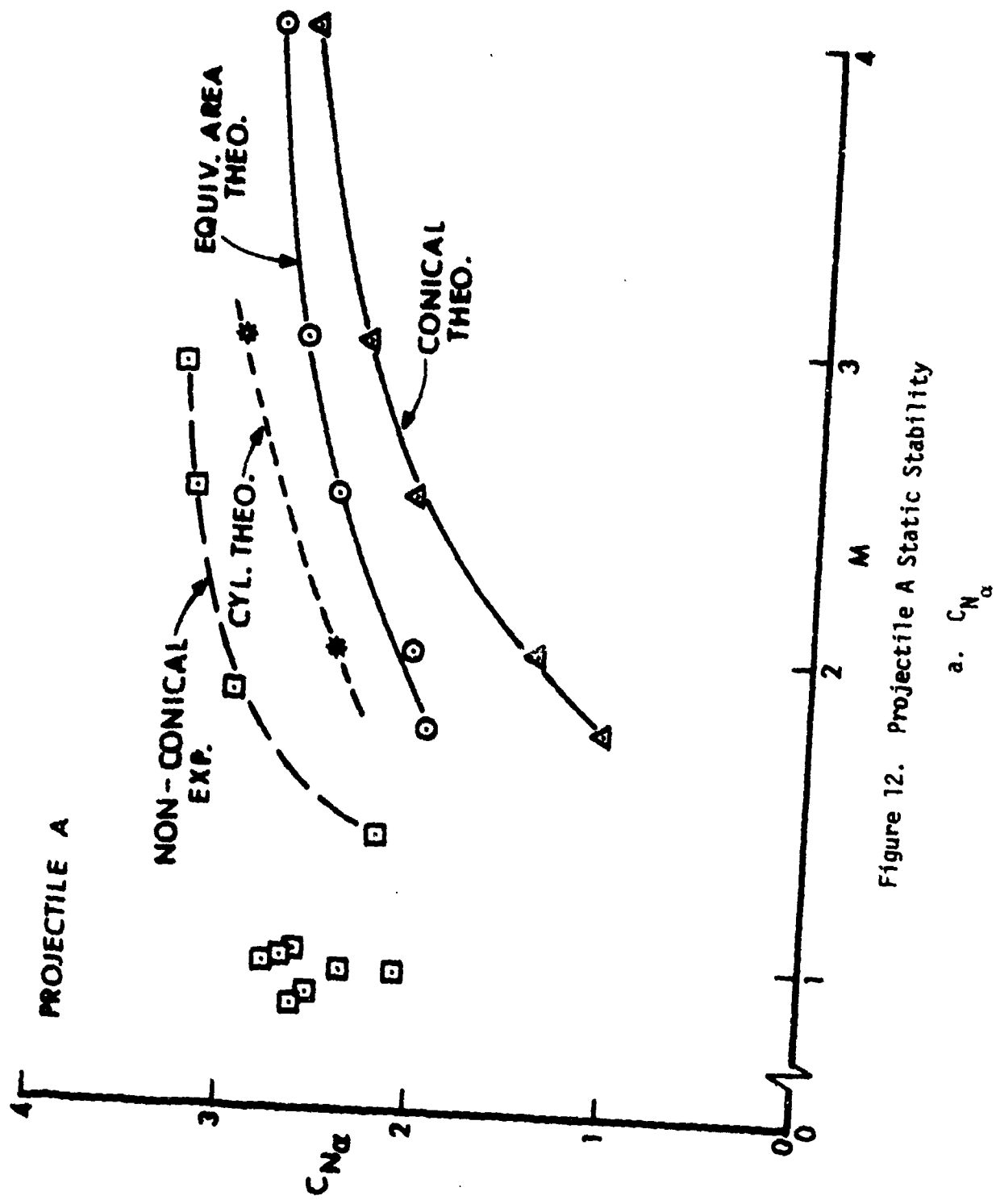


Figure 12. Projectile A Static Stability
a. $C_{N\alpha}$

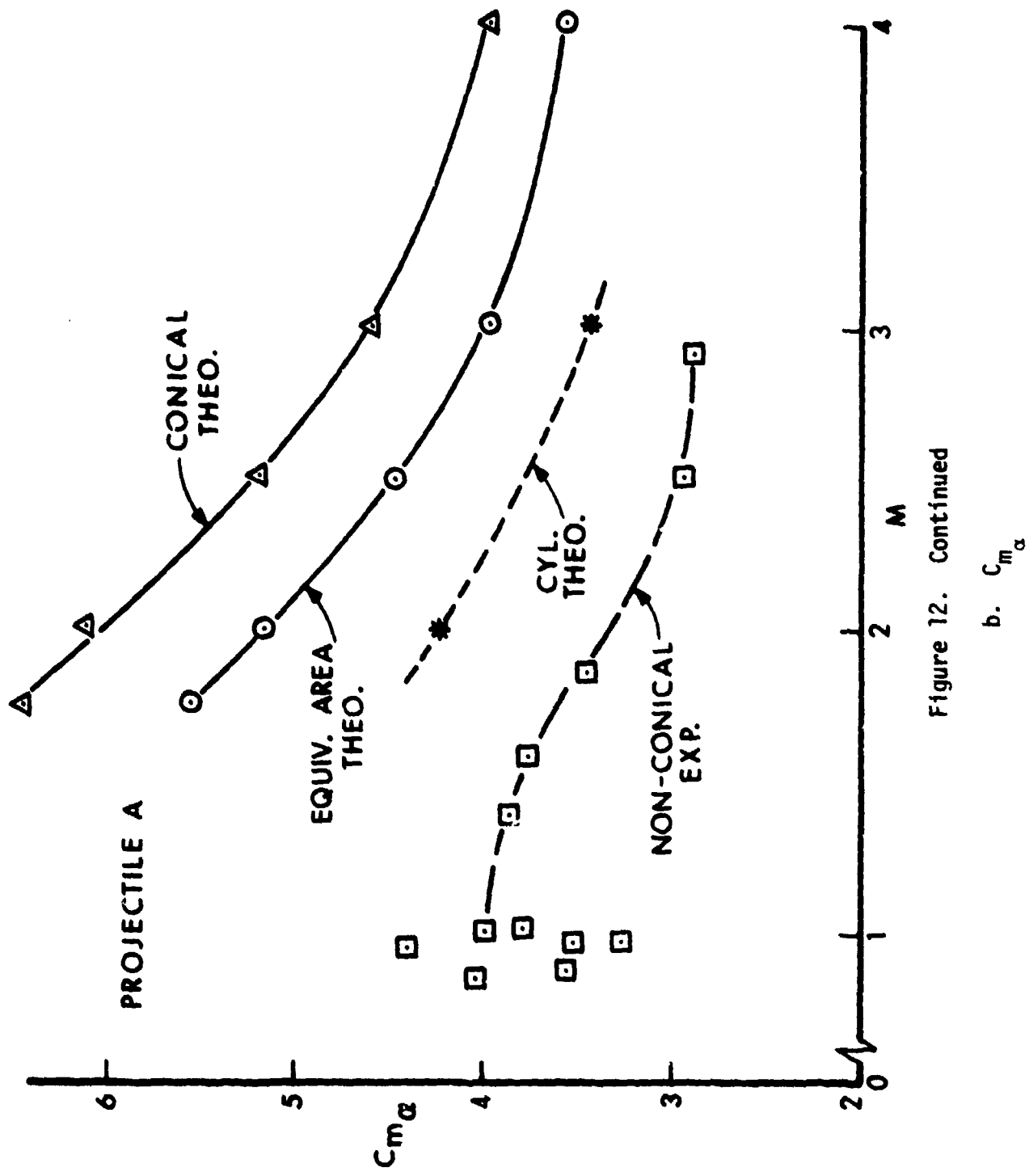


Figure 12. Continued

b. $C_{m\alpha}$

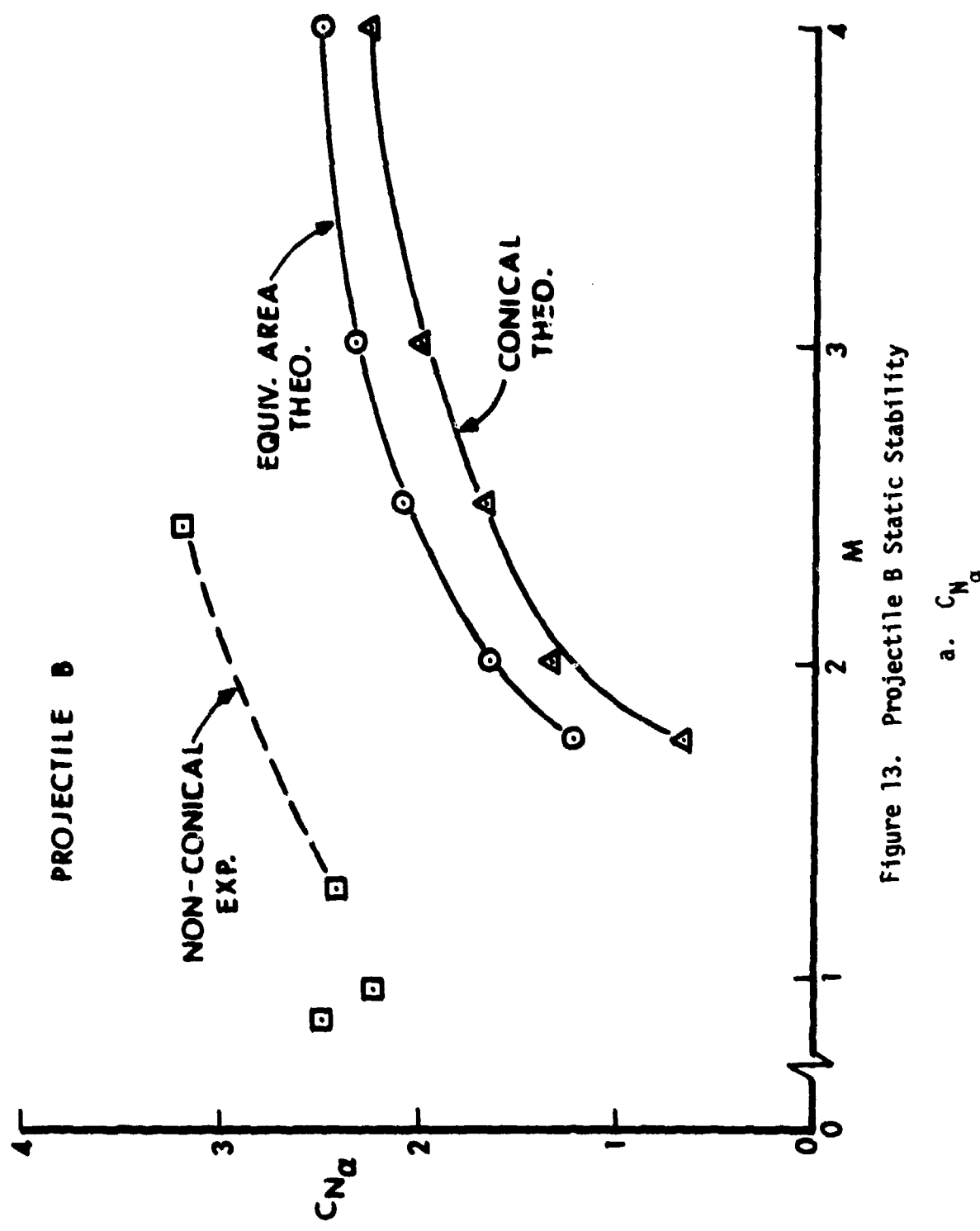


Figure 13. Projectile B Static Stability

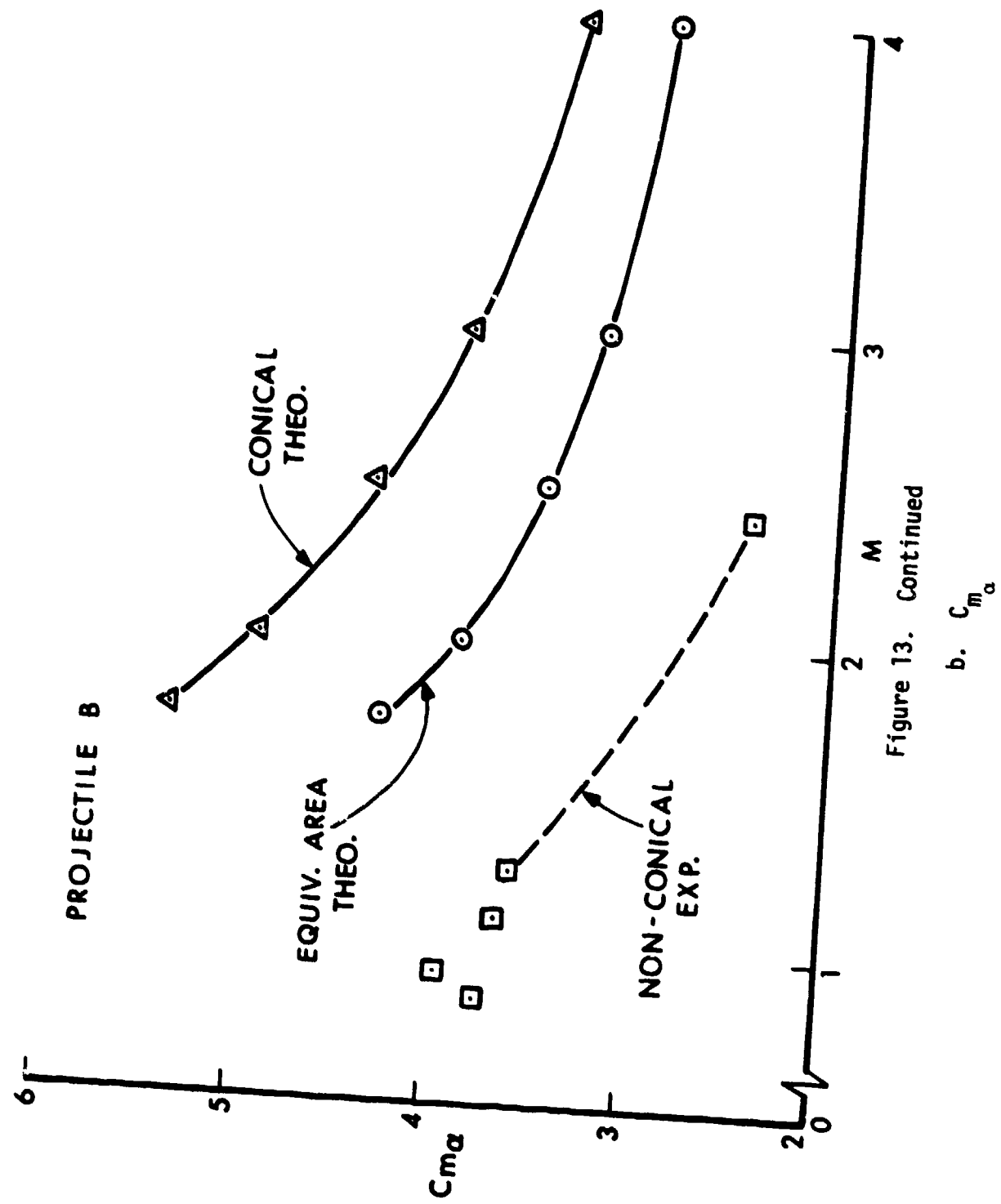


Figure 13. Continued

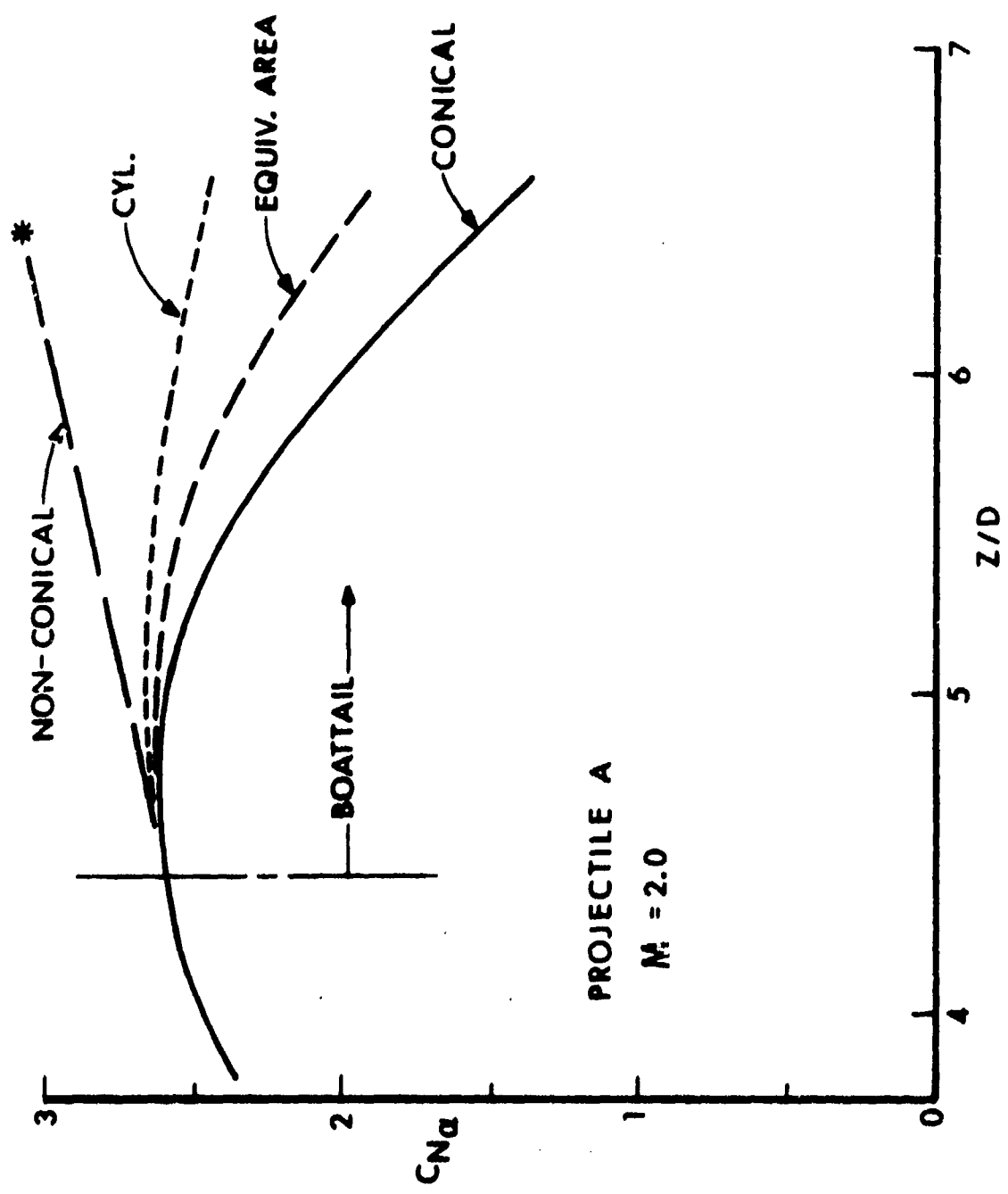


Figure 14. Effect of Boattail Length on the Performance of Projectile A

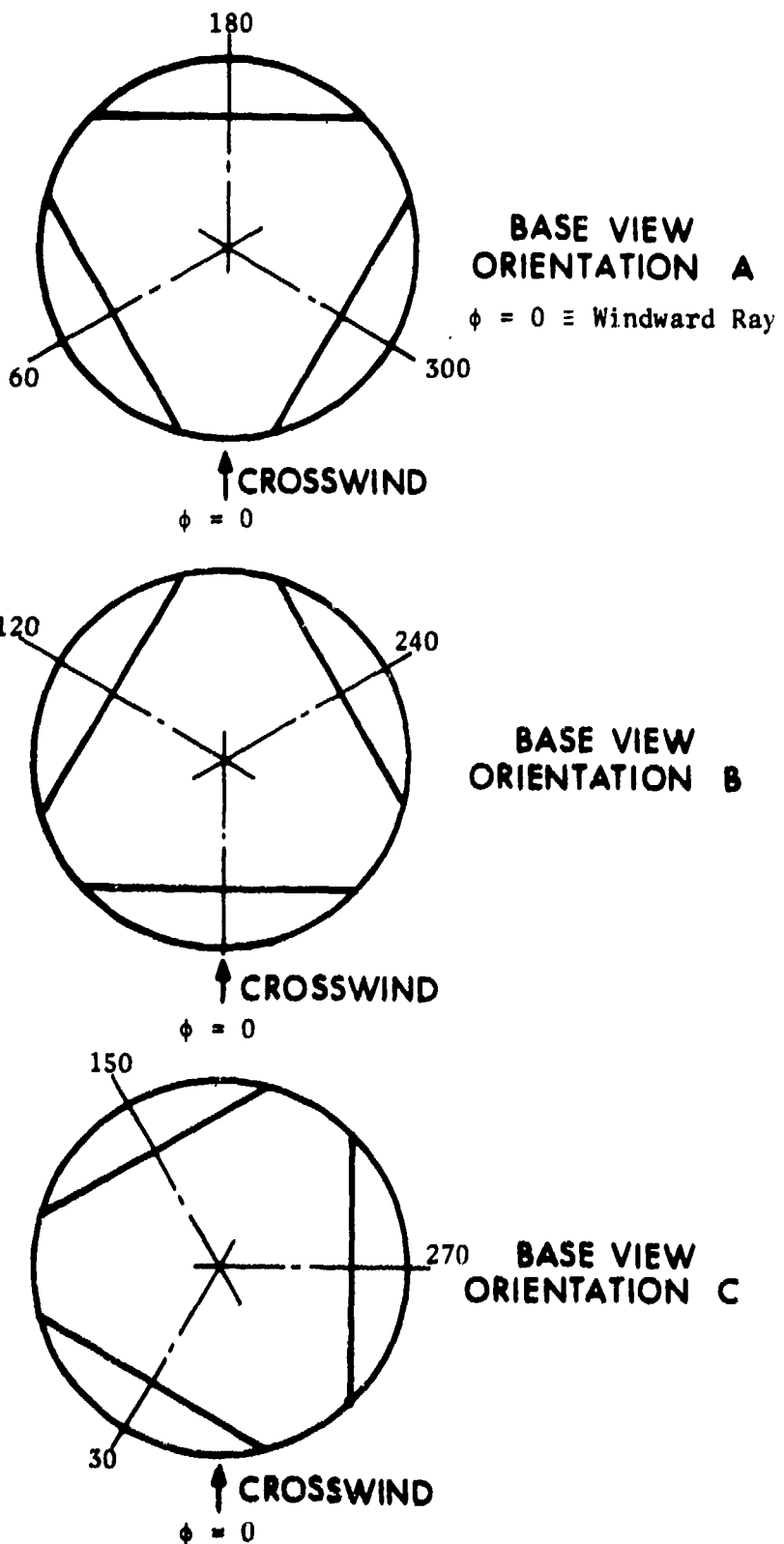
APPENDIX

Tabulated Pressure Data

CONTENTS

	<u>Page</u>
Model Orientation Sketch, SOCBT-NC
Summary of Tabulated Data
Tabulated Data

Model Orientation Sketch, SOCBT-NC



Summary of Tabulated Data

SOCBT-NC

<u>M_{∞}</u>	<u>Orientation</u>	<u>Page</u>
0.91	A	
0.91	B	
0.91	C	
1.75	A	
1.75	B	
1.75	C	
2.00	A	
2.00	B	
2.00	C	
3.02	A	
3.02	B	
3.02	C	

NOTE: P19, $Z/D = 5.75$, was in error; therefore, as an approximation, P19 was set equal to P18.

Tabulated Data

M=0.91 ORIENTATION A

Z/D	TAP	PHI	P/PS =0	P/PS =1.0	P/PS =2.5	P/PS =5.0
ALPHA	- - - - -	- - - - -				
5.25	17	0.0	.984	.980	.973	.977
5.25	14	49.6	.941	.932	.927	.922
5.25	8	60.0	.945	.947	.944	.943
5.25	11	70.4	.929	.925	.929	.936
5.25	17	120.0	.964	.972	.963	.956
5.25	14	169.6	.932	.940	.932	.932
5.25	8	180.0	.943	.936	.939	.951
5.25	11	190.4	.927	.939	.932	.932
5.25	17	240.0	.991	.997	.996	.996
5.25	14	289.6	.943	.945	.945	.947
5.25	8	300.0	.935	.945	.934	.926
5.25	11	310.4	.935	.935	.929	.921
5.50	18	0.0	.965	.957	.955	.961
5.50	15	44.7	.958	.948	.944	.940
5.50	9	60.0	.963	.964	.962	.960
5.50	12	75.3	.954	.949	.954	.959
5.50	18	120.0	.958	.968	.958	.951
5.50	15	164.7	.950	.959	.952	.950
5.50	9	180.0	.962	.956	.956	.966
5.50	12	194.3	.950	.964	.955	.954
5.50	18	240.0	.970	.971	.969	.967
5.50	15	284.7	.960	.962	.962	.962
5.50	9	300.0	.955	.965	.954	.947
5.50	12	315.3	.961	.960	.955	.948
5.75	19 *	0.0	.965	.957	.955	.961
5.75	16	40.5	1.003	1.003	.981	.973
5.75	10	60.0	.972	.973	.969	.967
5.75	13	79.5	.972	.971	.973	.977
5.75	19 *	120.0	.958	.968	.958	.951
5.75	16	160.5	.981	.977	.968	.968
5.75	10	180.0	.970	.963	.964	.971
5.75	13	199.5	.963	.975	.970	.967
5.75	19 *	240.0	.970	.971	.969	.967
5.75	16	280.5	.990	.991	.993	.995
5.75	10	300.0	.965	.973	.963	.954
5.75	13	319.5	.974	.976	.971	.966

*P19 ~ P18

Tabulated Data (Continued)

M=0.91 ORIENTATION B

Z/D	TAP	PHI	P/PS =0	P/PS =1.0	P/PS =2.5	P/PS =5.0
5.25	8	0.0	.935	.941	.935	.942
5.25	11	10.4	.936	.935	.935	.939
5.25	17	60.0	.971	.980	.974	.970
5.25	14	109.6	.931	.938	.929	.921
5.25	8	120.0	.947	.947	.946	.946
5.25	11	130.4	.924	.938	.938	.944
5.25	17	180.0	.955	.960	.969	.982
5.25	14	229.6	.931	.937	.936	.944
5.25	8	240.0	.934	.945	.942	.943
5.25	11	250.4	.928	.934	.926	.921
5.25	17	300.0	.982	.989	.990	.987
5.25	14	349.6	.941	.940	.939	.944
5.50	9	0.0	.955	.960	.956	.958
5.50	12	15.3	.961	.960	.958	.961
5.50	18	60.0	.957	.965	.959	.957
5.50	15	104.7	.949	.955	.947	.940
5.50	9	120.0	.964	.964	.964	.963
5.50	12	135.3	.948	.962	.962	.966
5.50	18	180.0	.959	.960	.957	.976
5.50	15	224.7	.950	.957	.957	.964
5.50	9	240.0	.954	.964	.961	.962
5.50	12	255.3	.952	.959	.951	.945
5.50	18	300.0	.971	.969	.965	.960
5.50	15	344.7	.960	.958	.957	.958
5.75	10	0.0	.966	.970	.964	.965
5.75	13	19.5	.971	.974	.973	.975
5.75	19*	60.0	.957	.965	.959	.957
5.75	16	100.5	.991	.995	.976	.971
5.75	10	120.0	.974	.973	.972	.972
5.75	13	139.5	.964	.978	.978	.984
5.75	19*	180.0	.959	.960	.967	.976
5.75	16	220.5	.963	.957	.967	.981
5.75	10	240.0	.963	.972	.970	.969
5.75	13	259.5	.962	.967	.965	.963
5.75	19*	180.0	.971	.969	.965	.960
5.75	16	340.5	.975	.978	.984	.988

*P19 ≈ P18

Tabulated Data (Continued)

M=0.91 ORIENTATION C

Z/D	TAP	PHI	P/PS =0	P/PS =1.0	P/PS =2.5	P/PS =5.0
5.25	14	19.6	.940	.939	.936	.937
5.25	8	30.0	.943	.945	.943	.946
5.25	11	40.4	.937	.940	.939	.943
5.25	17	90.0	.970	.976	.971	.966
5.25	14	139.6	.932	.939	.933	.933
5.25	8	150.0	.947	.949	.949	.951
5.25	11	160.4	.927	.939	.939	.945
5.25	17	210.0	.994	.999	.998	1.005
5.25	14	259.6	.943	.946	.945	.948
5.25	8	270.0	.935	.945	.940	.938
5.25	11	280.4	.934	.936	.927	.917
5.25	17	330.0	.977	.986	.988	.991
5.50	15	14.7	.959	.959	.954	.954
5.50	9	30.0	.962	.965	.960	.962
5.50	12	44.3	.961	.963	.961	.964
5.50	18	90.0	.959	.966	.960	.955
5.50	15	134.7	.951	.956	.951	.950
5.50	9	150.0	.964	.967	.966	.967
5.50	12	165.3	.950	.964	.962	.968
5.50	18	210.0	.968	.973	.971	.975
5.50	15	254.7	.959	.963	.962	.965
5.50	9	270.0	.956	.964	.959	.957
5.50	12	285.3	.959	.960	.953	.945
5.50	18	330.0	.969	.970	.965	.964
5.75	16	10.5	.966	.974	.979	.981
5.75	10	30.0	.970	.972	.967	.967
5.75	13	49.5	.970	.976	.976	.979
5.75	19*	90.0	.959	.966	.960	.955
5.75	16	130.5	.989	.985	.974	.974
5.75	10	150.0	.974	.975	.973	.973
5.75	13	169.5	.964	.976	.977	.984
5.75	19*	210.0	.968	.973	.971	.975
5.75	16	250.5	.997	.996	.995	.999
5.75	10	270.0	.966	.973	.968	.967
5.75	13	289.5	.975	.978	.970	.965
5.75	19*	330.0	.969	.970	.965	.964

*P19 ~ P18

Tabulated Data (Continued)

M=1.75 ORIENTATION A

Z/D	TAP	PHI	P/PS ≈0	P/PS ≈1.0	P/PS ≈2.5	P/PS ≈5.0
ALPHA- - - - - - - -						
5.25	17	0.0	.918	.918	.925	.949
5.25	14	49.6	.730	.718	.694	.645
5.25	8	60.0	.746	.743	.731	.705
5.25	11	70.4	.723	.729	.731	.725
5.25	17	120.0	.920	.913	.915	.890
5.25	14	169.6	.740	.744	.761	.779
5.25	8	180.0	.764	.771	.785	.801
5.25	11	190.4	.740	.745	.757	.777
5.25	17	240.0	.918	.907	.922	.899
5.25	14	289.6	.736	.736	.744	.730
5.25	8	300.0	.753	.746	.733	.704
5.25	11	310.4	.717	.702	.667	.615
5.50	18	0.0	.900	.905	.915	.937
5.50	15	44.7	.766	.758	.741	.704
5.50	9	60.0	.776	.774	.765	.759
5.50	12	75.3	.766	.767	.772	.758
5.50	18	120.0	.914	.905	.906	.855
5.50	15	164.7	.776	.778	.790	.800
5.50	9	180.0	.790	.796	.818	.826
5.50	12	194.3	.778	.780	.798	.808
5.50	18	240.0	.907	.903	.903	.861
5.50	15	284.7	.770	.771	.778	.780
5.50	9	300.0	.786	.783	.786	.760
5.50	12	315.3	.768	.759	.739	.687
5.75	19*	0.0	.900	.905	.915	.937
5.75	16	40.5	.789	.781	.775	.753
5.75	10	60.0	.800	.804	.814	.787
5.75	13	79.5	.784	.799	.818	.805
5.75	19*	120.0	.914	.906	.906	.855
5.75	16	160.5	.789	.795	.811	.807
5.75	10	180.0	.813	.819	.839	.838
5.75	13	199.5	.792	.796	.814	.811
5.75	19*	240.0	.907	.903	.903	.861
5.75	16	280.5	.813	.801	.822	.805
5.75	10	300.0	.805	.807	.812	.780
5.75	13	319.5	.785	.776	.766	.731

*P19 ≈ P18

Tabulated Data (Continued)

M=1.75 ORIENTATION B

Z/D	TAP	PHI	P/PS =0	P/PS =1.0	P/PS =2.5	P/PS =5.0
ALPHA- - - - -						
5.25	8	0.0	.745	.741	.739	.745
5.25	11	10.4	.717	.715	.714	.723
5.25	17	60.0	.919	.915	.913	.901
5.25	14	109.6	.729	.716	.700	.649
5.25	8	120.0	.753	.753	.754	.742
5.25	11	130.4	.736	.743	.759	.765
5.25	17	180.0	.953	.930	.948	.947
5.25	14	229.6	.748	.753	.772	.780
5.25	8	240.0	.761	.762	.768	.758
5.25	11	250.4	.722	.712	.702	.656
5.25	17	300.0	.881	.887	.901	.866
5.25	14	349.6	.726	.724	.725	.733
5.50	9	0.0	.773	.772	.771	.767
5.50	12	15.3	.757	.755	.754	.761
5.50	18	60.0	.907	.909	.918	.910
5.50	15	104.7	.755	.768	.735	.687
5.50	9	120.0	.784	.783	.790	.777
5.50	12	135.3	.777	.800	.801	.804
5.50	18	180.0	.909	.907	.915	.893
5.50	15	224.7	.777	.781	.800	.805
5.50	9	240.0	.789	.789	.797	.790
5.50	12	255.3	.763	.758	.746	.710
5.50	18	300.0	.910	.914	.925	.894
5.50	15	344.7	.764	.764	.765	.711
5.75	10	0.0	.796	.800	.803	.810
5.75	13	19.5	.771	.777	.789	.800
5.75	19*	60.0	.907	.909	.918	.910
5.75	16	100.5	.783	.784	.774	.719
5.75	10	120.0	.804	.800	.813	.801
5.75	13	139.5	.793	.798	.820	.820
5.75	19*	180.0	.909	.907	.915	.893
5.75	15	220.5	.863	.831	.839	.835
5.75	10	240.0	.808	.805	.821	.813
5.75	13	259.5	.799	.796	.783	.718
5.75	19*	180.0	.910	.914	.925	.894
5.75	16	340.5	.762	.766	.784	.795

*P19 ≈ P18

Tabulated Data (Continued)

M=1.75 ORIENTATION C

Z/D	TAP	PHI	P/PS =0	P/PS =1.0	P/PS =2.5	P/PS =5.0
5.25	14	19.6	.723	.717	.711	.703
5.25	8	30.0	.746	.743	.738	.733
5.25	11	40.4	.721	.722	.726	.731
5.25	17	90.0	.920	.912	.908	.870
5.25	14	139.6	.734	.727	.735	.737
5.25	8	150.0	.758	.763	.771	.781
5.25	11	160.4	.740	.748	.766	.780
5.25	17	210.0	.935	.917	.935	.930
5.25	14	259.6	.743	.746	.757	.742
5.25	8	270.0	.756	.752	.745	.709
5.25	11	280.4	.718	.703	.672	.592
5.25	17	330.0	.866	.883	.898	.905
5.50	15	14.7	.758	.754	.748	.740
5.50	9	30.0	.774	.773	.771	.768
5.50	12	44.3	.763	.763	.768	.783
5.50	18	90.0	.911	.906	.905	.850
5.50	15	134.7	.774	.769	.765	.759
5.50	9	150.0	.787	.790	.806	.804
5.50	12	165.3	.778	.782	.804	.813
5.50	18	210.0	.910	.907	.913	.896
5.50	15	254.7	.771	.774	.790	.782
5.50	9	270.0	.785	.782	.782	.758
5.50	12	285.3	.762	.753	.731	.665
5.50	18	330.0	.912	.915	.923	.923
5.75	16	10.5	.740	.754	.769	.775
5.75	10	30.0	.797	.801	.799	.801
5.75	13	49.5	.769	.782	.795	.799
5.75	19*	90.0	.911	.906	.905	.850
5.75	16	130.5	.786	.793	.790	.773
5.75	10	150.0	.808	.806	.825	.816
5.75	13	169.5	.794	.799	.824	.827
5.75	19*	210.0	.910	.907	.913	.886
5.75	16	250.5	.835	.811	.830	.829
5.75	10	270.0	.803	.806	.819	.792
5.75	13	289.5	.794	.790	.765	.684
5.75	19*	330.0	.912	.915	.923	.923

*P19 ≈ P18

Tabulated Data (Continued)

Ma 2.02 ORIENTATION A

Z/D	TAP	PHI	P/PS =0	P/PS =1.0	P/PS =2.5	P/PS =5.0
ALPHA=	- - - - -	- - - - -	- - - - -	- - - - -	- - - - -	- - - - -
5.25	17	0.0	.949	.951	.960	.990
5.25	14	49.6	.738	.722	.693	.644
5.25	9	60.0	.748	.743	.729	.694
5.25	11	70.4	.730	.736	.736	.725
5.25	17	120.0	.922	.935	.937	.896
5.25	14	169.6	.729	.734	.742	.772
5.25	8	180.0	.762	.760	.769	.792
5.25	11	190.4	.729	.732	.740	.767
5.25	17	240.0	.931	.923	.924	.888
5.25	14	289.6	.736	.740	.743	.726
5.25	8	300.0	.759	.751	.733	.696
5.25	11	310.4	.720	.701	.667	.609
5.50	18	0.0	.949	.958	.972	1.000
5.50	15	44.7	.771	.760	.735	.659
5.50	9	60.0	.780	.776	.764	.739
5.50	12	75.3	.769	.771	.780	.768
5.50	18	120.0	.945	.935	.943	.888
5.50	15	164.7	.768	.773	.779	.799
5.50	9	180.0	.792	.790	.810	.822
5.50	12	194.3	.769	.772	.787	.803
5.50	18	240.0	.936	.929	.940	.893
5.50	15	284.7	.768	.771	.780	.765
5.50	9	300.0	.799	.784	.771	.742
5.50	12	315.3	.765	.752	.719	.620
5.75	19*	0.0	.949	.958	.972	1.000
5.75	16	40.5	.806	.776	.753	.728
5.75	10	60.0	.804	.798	.794	.777
5.75	13	79.5	.795	.780	.811	.800
5.75	19*	120.0	.945	.935	.943	.888
5.75	16	160.5	.763	.780	.805	.810
5.75	10	180.0	.812	.804	.838	.844
5.75	13	199.5	.782	.785	.812	.815
5.75	19*	240.0	.936	.929	.940	.893
5.75	16	280.5	.801	.806	.820	.813
5.75	10	300.0	.814	.808	.807	.780
5.75	13	319.5	.785	.781	.756	.727

*P19 ≈ P18

Tabulated Data (Continued)

M=2.02 ORIENTATION 3

Z/D	TAP	PHI	P/PS =0	P/PS =1.0	P/PS =2.5	P/PS =5.0
5.25	8	0.0	.749	.745	.745	.759
5.25	11	10.4	.722	.716	.717	.735
5.25	17	60.0	.935	.948	.943	.910
5.25	14	109.6	.730	.716	.683	.618
5.25	8	120.0	.748	.747	.738	.718
5.25	11	130.4	.736	.740	.748	.755
5.25	17	180.0	.961	.940	.959	.952
5.25	14	229.6	.741	.748	.757	.766
5.25	8	240.0	.758	.757	.748	.737
5.25	11	250.4	.717	.704	.670	.618
5.25	17	300.0	.920	.917	.918	.879
5.25	14	349.6	.732	.729	.731	.748
5.50	9	0.0	.780	.775	.773	.790
5.50	12	15.3	.767	.757	.757	.774
5.50	18	60.0	.951	.953	.954	.927
5.50	15	104.7	.769	.761	.723	.634
5.50	9	120.0	.778	.778	.779	.762
5.50	12	135.3	.772	.772	.793	.802
5.50	18	180.0	.934	.922	.949	.928
5.50	15	224.7	.769	.773	.795	.804
5.50	9	240.0	.788	.788	.791	.783
5.50	12	255.3	.757	.758	.723	.667
5.50	18	300.0	.943	.942	.950	.912
5.50	15	344.7	.767	.763	.766	.781
5.75	10	0.0	.801	.801	.802	.811
5.75	13	19.5	.782	.780	.783	.797
5.75	19*	60.0	.951	.953	.954	.927
5.75	16	100.5	.777	.775	.749	.624
5.75	10	120.0	.800	.801	.810	.796
5.75	13	139.5	.793	.794	.823	.828
5.75	19*	180.0	.934	.922	.949	.929
5.75	16	220.5	.836	.829	.847	.856
5.75	10	240.0	.810	.807	.820	.809
5.75	13	259.5	.791	.783	.762	.630
5.75	19*	180.0	.943	.942	.950	.912
5.75	16	340.5	.775	.776	.782	.804

*P19 ~ P18

Tabulated Data (Continued)

M=2.02 ORIENTATION C

Z/D	TAP	PHI	P/PS =20	P/PS =1.0	P/PS =2.5	P/PS =5.0
5.25	14	19.6	.729	.720	.713	.712
5.25	8	30.0	.749	.744	.741	.744
5.25	11	40.4	.723	.725	.730	.741
5.25	17	90.0	.931	.942	.934	.873
5.25	14	139.6	.730	.724	.713	.719
5.25	8	150.0	.746	.752	.753	.767
5.25	11	160.4	.734	.738	.745	.774
5.25	17	210.0	.939	.929	.945	.932
5.25	14	259.6	.738	.744	.748	.732
5.25	8	270.0	.758	.754	.739	.691
5.25	11	280.4	.718	.699	.652	.563
5.25	17	330.0	.909	.913	.922	.929
5.50	15	14.7	.765	.758	.751	.746
5.50	9	30.0	.781	.777	.774	.777
5.50	12	44.3	.769	.762	.767	.775
5.50	18	90.0	.949	.944	.946	.882
5.50	15	134.7	.769	.767	.746	.748
5.50	9	150.0	.778	.783	.793	.796
5.50	12	165.3	.772	.772	.795	.812
5.50	18	210.0	.937	.924	.947	.917
5.50	15	254.7	.768	.771	.788	.779
5.50	9	270.0	.788	.786	.781	.743
5.50	12	285.3	.761	.753	.704	.595
5.50	18	330.0	.944	.948	.956	.961
5.75	16	10.5	.761	.759	.762	.769
5.75	10	30.0	.803	.802	.800	.797
5.75	13	49.5	.781	.785	.791	.802
5.75	19*	90.0	.949	.944	.946	.882
5.75	16	130.5	.771	.777	.775	.759
5.75	10	150.0	.800	.803	.821	.817
5.75	13	169.5	.789	.790	.820	.832
5.75	19*	210.0	.937	.924	.947	.917
5.75	16	250.5	.812	.816	.835	.834
5.75	10	270.0	.811	.808	.813	.777
5.75	13	289.5	.785	.782	.744	.617
5.75	19*	330.0	.944	.948	.956	.961

*P19 ~ P18

Tabulated Data (Continued)

M=3.02 ORIENTATION A

Z/D	TAP	PHI	P/PS ≈0	P/PS ≈1.0	P/PS ≈2.5	P/PS ≈5.0
5.25	17	0.0	.966	.983	.920	1.042
5.25	14	49.6	.640	.622	.542	.554
5.25	8	60.0	.643	.636	.620	.605
5.25	11	70.4	.627	.627	.632	.604
5.25	17	120.0	.915	.870	.828	.698
5.25	14	169.6	.649	.661	.642	.621
5.25	8	180.0	.668	.680	.648	.679
5.25	11	190.4	.648	.663	.650	.671
5.25	17	240.0	.974	.873	.853	.789
5.25	14	289.6	.631	.625	.621	.603
5.25	8	300.0	.645	.640	.625	.586
5.25	11	310.4	.625	.611	.582	.536
5.50	18	0.0	.897	.910	.954	1.035
5.50	15	44.7	.624	.603	.577	.529
5.50	9	60.0	.653	.642	.636	.632
5.50	12	75.3	.617	.624	.615	.613
5.50	18	120.0	.884	.866	.831	.742
5.50	15	164.7	.627	.627	.613	.616
5.50	9	180.0	.665	.662	.667	.693
5.50	12	194.3	.631	.630	.644	.649
5.50	18	240.0	.884	.866	.859	.802
5.50	15	284.7	.623	.627	.623	.588
5.50	9	300.0	.636	.628	.605	.546
5.50	12	315.3	.591	.579	.543	.504
5.75	19*	0.0	.897	.910	.964	1.035
5.75	16	40.5	.699	.675	.566	.600
5.75	10	60.0	.645	.643	.631	.616
5.75	13	79.5	.630	.647	.646	.641
5.75	19*	120.0	.884	.866	.831	.742
5.75	16	160.5	.644	.573	.551	.618
5.75	10	180.0	.659	.663	.698	.701
5.75	13	199.5	.615	.594	.640	.667
5.75	19*	240.0	.884	.866	.859	.802
5.75	16	280.5	.761	.639	.643	.611
5.75	10	300.0	.641	.634	.614	.563
5.75	13	319.5	.629	.567	.522	.466

*P19 ≈ P18

Tabulated Data (Continued)

M=3.02 ORIENTATION B

Z/D	TAP	PHI	P/PS =0	P/PS =1.0	P/PS =2.5	P/PS =5.0
5.25	8	0.0	.668	.661	.657	.681
5.25	11	10.4	.638	.632	.630	.664
5.25	17	60.0	.948	.635	.925	.864
5.25	14	109.6	.639	.623	.577	.471
5.25	8	120.0	.645	.646	.616	.525
5.25	11	130.4	.631	.637	.623	.572
5.25	17	180.0	.933	.876	.895	.886
5.25	14	229.6	.664	.669	.641	.601
5.25	8	240.0	.662	.658	.618	.548
5.25	11	250.4	.620	.603	.552	.457
5.25	17	300.0	.989	.896	.890	.871
5.25	14	349.6	.662	.649	.658	.692
5.50	9	0.0	.665	.646	.644	.649
5.50	12	15.3	.606	.618	.633	.678
5.50	18	60.0	.893	.905	.915	.911
5.50	15	104.7	.613	.586	.527	.426
5.50	9	120.0	.646	.637	.601	.512
5.50	12	135.3	.624	.634	.622	.599
5.50	18	180.0	.810	.845	.871	.847
5.50	15	224.7	.642	.644	.628	.630
5.50	9	240.0	.654	.655	.633	.561
5.50	12	255.3	.602	.592	.520	.412
5.50	18	300.0	.873	.870	.851	.794
5.50	15	344.7	.638	.637	.656	.709
5.75	10	0.0	.659	.668	.677	.710
5.75	13	19.5	.646	.622	.637	.688
5.75	19*	60.0	.893	.905	.915	.911
5.75	16	100.5	.666	.587	.497	.421
5.75	10	120.0	.640	.645	.607	.511
5.75	13	139.5	.630	.642	.654	.654
5.75	19*	180.0	.810	.845	.871	.847
5.75	16	220.5	.729	.642	.678	.687
5.75	10	240.0	.651	.652	.638	.569
5.75	13	259.5	.609	.533	.462	.384
5.75	19*	180.0	.873	.870	.851	.794
5.75	16	340.5	.818	.660	.669	.726

*P19 ≈ P18

Tabulated Data (Continued)

M=3.02 ORIENTATION C

Z/D	TAP	PHI	P/PS =0	P/PS =1.0	P/PS =2.5	P/PS =5.0
ALPHA	- - - - -	- - - - -	- - - - -	- - - - -	- - - - -	- - - - -
5.25	14	19.6	.654	.626	.621	.652
5.25	8	30.0	.651	.646	.635	.667
5.25	11	40.4	.621	.625	.633	.669
5.25	17	90.0	.939	.909	.878	.763
5.25	14	139.6	.640	.638	.601	.536
5.25	8	150.0	.649	.661	.620	.609
5.25	11	160.4	.636	.651	.633	.638
5.25	17	210.0	.971	.899	.892	.888
5.25	14	259.6	.629	.630	.598	.546
5.25	8	270.0	.634	.622	.592	.514
5.25	11	280.4	.597	.580	.537	.439
5.25	17	330.0	1.028	.940	.962	1.008
5.50	15	14.7	.642	.627	.623	.646
5.50	9	30.0	.660	.651	.654	.681
5.50	12	44.3	.602	.619	.632	.681
5.50	18	90.0	.884	.882	.863	.792
5.50	15	134.7	.617	.602	.543	.451
5.50	9	150.0	.652	.655	.625	.581
5.50	12	165.3	.629	.640	.641	.665
5.50	18	210.0	.893	.866	.917	.888
5.50	15	254.7	.622	.625	.618	.566
5.50	9	270.0	.640	.633	.605	.523
5.50	12	285.3	.585	.572	.479	.396
5.50	18	330.0	.902	.924	.949	1.000
5.75	16	10.5	.821	.643	.635	.657
5.75	10	30.0	.656	.661	.652	.683
5.75	13	49.5	.646	.632	.654	.693
5.75	19*	90.0	.884	.882	.863	.792
5.75	16	130.5	.652	.574	.480	.404
5.75	10	150.0	.651	.665	.662	.662
5.75	13	169.5	.631	.636	.675	.711
5.75	19*	210.0	.893	.866	.917	.888
5.75	16	250.5	.747	.642	.653	.610
5.75	10	270.0	.642	.635	.609	.499
5.75	13	28.5	.608	.523	.456	.373
5.75	19*	330.0	.902	.924	.949	1.000

*P19 ≈ P18

LIST OF SYMBOLS

ALPHA - angle of attack, degree

$C_{m\alpha}$ - slope of the pitching moment curve at $\alpha = 0$, 1/rad.

$C_{N\alpha}$ - slope of the normal force coefficient curve at $\alpha = 0$, 1/rad.

M - Mach number

p, P - model wall pressure

PHI - circumferential position on the model, 0 = wind side,
180 = lee side

P_0 - tunnel supply pressure, atm.

P_S, P_∞ - free-stream static pressure

Re_ℓ - Reynolds number base on model length

T_0 - tunnel supply pressure, °K

Z/D - distance from model nose, calibers

α - angle of attack, degree

ϕ - circumferential position on the model, 0 = wind side,
180 = lee side

PRINTING PAGE BLANK - NOT FILMED

DISTRIBUTION LIST

<u>No. of Copies</u>	<u>Organization</u>	<u>No. of Copies</u>	<u>Organization</u>
12	<p>Commander Defense Technical Info Center ATTN: DDC-DDA Cameron Station Alexandria, VA 22314</p>	1	<p>Director US Army Air Mobility Research and Development Laboratory Ames Research Center Moffett Field, CA 94035</p>
1	<p>Commander US Army Materiel Development and Readiness Command ATTN: DRCDMD-ST 5001 Eisenhower Avenue Alexandria, VA 22333</p>	1	<p>Commander US Army Communications Research and Development Command ATTN: DRDCO-PPA-SA Fort Monmouth, NJ 07703</p>
8	<p>Commander US Army Armament Research and Development Command ATTN: DRDAR-TSS (2 cys) DRDAR-LCA-F Mr. D. Mertz Mr. E. Falkowski Mr. A. Loeb Mr. R. Kline Mr. S. Kahn Mr. S. Wasserman Dover, NJ 07801</p>	1	<p>Commander US Army Electronics Research and Development Command Technical Support Activity ATTN: DELSD-L Fort Monmouth, NJ 07703</p>
1	<p>Commander US Army Armament Materiel Readiness Command ATTN: DRSAR-LEP-L, Tech Lib Rock Island, IL 61299</p>	3	<p>Commander US Army Missile Command ATTN: DRSMI-R DRDMI-YDL DRSMI-RDK Mr. R. Deep Redstone Arsenal, AL 35809</p>
1	<p>Director US Army Armament Research and Development Command Benet Weapons Laboratory ATTN: DRDAR-LCB-TL Watervliet, NY 12189</p>	1	<p>Commander US Army Tank Automotive Research and Development Command ATTN: DRDTA-UL Warren, MI 48090</p>
1	<p>Commander US Army Aviation Research and Development Command ATTN: DRSAV-E P. O. Box 209 St. Louis, MO 61366</p>	1	<p>Director US Army TRADOC Systems Analysis Activity ATTN: ATAA-SL, Tech Lib White Sands Missile Range NM 88002</p>

DISTRIBUTION LIST

<u>No. of Copies</u>	<u>Organization</u>	<u>No. of Copies</u>	<u>Organization</u>
1	Commander US Army Research Office P. O. Box 12211 Research Triangle Park NC 27709	1	Director NASA Langley Research Center ATTN: MS-185, Tech Lib Langley Station Hampton, VA 23365
1	Commander US Naval Air Systems Command ATTN: AIR-604 Washington, D. C. 20360	1	Director NASA Ames Research Center ATTN: MS-202, Tech Lib Moffett Field, CA 94035
2	Commander David W. Taylor Naval Ship Research and Development Center ATTN: Dr. S. de los Santos Mr. Stanley Gottlieb Bethesda, Maryland 20084	1	Arnold Research Organization, Inc. von Karman Gas Dynamics Facility ATTN: Dr. John C. Adams, Jr. Aerodynamics Division Projects Branch Arnold AFS, TN 37389
4	Commander US Naval Surface Weapons Center ATTN: Dr. T. Clare, Code DK20 Dr. P. Daniels Mr. D. A. Jones III Mr. L. Mason Dahlgren, VA 22448	1	Flow Simulations, Inc. ATTN: Dr. J. Steger 735 Alice Avenue Mountain View, CA 94041
3	Commander US Naval Surface Weapons Center ATTN: Code 312 Mr. R. Voisinet Mr. R. Driftmeyer Mr. R. Schlie Silver Spring, MD 20910	1	Sandia Laboratories ATTN: Division No. 1331 Mr. H. R. Vaughn P. O. Box 580 Albuquerque, NM 87115
1	Commander US Naval Weapons Center ATTN: Technical Library China Lake, CA 93555	2	Massachusetts Institute of Technology ATTN: Prof. E. Covert Prof. C. Haldeman 77 Massachusetts Avenue Cambridge, MA 02139
		1	University of Delaware Mechanical and Aerospace Engineering Department ATTN: Dr. James E. Danberg Newark, DE 19711

DISTRIBUTION LIST

<u>No. of Copies</u>	<u>Organization</u>
1	New York University Antonic Ferri Aerospace and Energetics Laboratory ATTN: Prof. V. Zakkay Merrick & Stewart Avenues Westberg, New York 11590
1	Virginia Polytechnic Institute and State University Department of Aerospace and Ocean Engineering ATTN: Prof. George R. Inger Blacksburg, VA 24061

Aberdeen Proving Ground

Director, USAMSAA
ATTN: DRXSY-D
DRXSY-MP, H. Cohen

Commander, USATECOM
ATTN: DRSTE-TO-F

Director, Weapons System
Concepts Team,
Bldg, E3516, EA
ATTN: DRDAR-ACW
Mr. M. Miller

USER EVALUATION OF REPORT

Please take a few minutes to answer the questions below; tear out this sheet and return it to Director, US Army Ballistic Research Laboratory, ARRADCOM, ATTN: DRDAR-TSB, Aberdeen Proving Ground, Maryland 21005. Your comments will provide us with information for improving future reports.

1. BRL Report Number _____

2. Does this report satisfy a need? (Comment on purpose, related project, or other area of interest for which report will be used.)

3. How, specifically, is the report being used? (Information source, design data or procedure, management procedure, source of ideas, etc.)

4. Has the information in this report led to any quantitative savings as far as man-hours/contract dollars saved, operating costs avoided, efficiencies achieved, etc.? If so, please elaborate.

5. General Comments (Indicate what you think should be changed to make this report and future reports of this type more responsive to your needs, more usable, improve readability, etc.)

6. If you would like to be contacted by the personnel who prepared this report to raise specific questions or discuss the topic, please fill in the following information.

Name: _____

Telephone Number: _____

Organization Address: _____

